Canonical Wnt/β-catenin Activity and Differential Epigenetic Marks Direct Sexually Dimorphic Regulation of *Irx3* and *Irx5* in Developing Gonads

Megan L Koth[1§]; S. Alexandra Garcia-Moreno[5§]; Annie Novak[1]; Kirsten A. Holthusen[2]; Anbarasi Kothandapani[1]; Keer Jiang[1]; Makoto Mark Taketo[3]; Barbara Nicol[4]; Humphrey H-C Yao[4]; Christopher R. Futtner[5]; Danielle M. Maatouk[5 †]; Joan S. Jorgensen[1*]

[1]Department of Comparative Biosciences, School of Veterinary Medicine, University of
Wisconsin – Madison, Madison, Wisconsin, USA

[2]Department of Comparative Biosciences, College of Veterinary Medicine, University of Illinois, Urbana, Illinois, USA

[3]Department of Pharmacology, Kyoto University Graduate School of Medicine, Kyoto Japan

[4]Reproductive and Developmental Biology Laboratory, National Institute of Environmental Health Sciences, Research Triangle Park, North Carolina, USA

[5]Department of Obstetrics and Gynecology, Northwestern University, Chicago, Illinois,
USA.

*Current location: Department of Cell Biology, Duke University Medical Center.

§ These authors have equal contributions

† Deceased

*Corresponding author

Summary Statement

Differential occupation of two enhancers define sex-specific regulation of *Irx3* and *Irx5* in fetal gonads: repressor marks inhibit in testes while active marks engage with β-catenin/TCF to stimulate in ovaries.

Abstract

Members of the Iroquois B (*IrxB*) homeodomain cluster genes, specifically *Irx3* and *Irx5*, are critical for heart, limb, and bone development. Recently, we reported their importance for oocyte and follicle survival within the developing ovary. *Irx3* and *Irx5* expression begins after sex determination in the ovary but remains absent in the fetal testis. Mutually antagonistic molecular signals ensure ovary vs testis differentiation with canonical Wnt/β-catenin signals paramount for promoting the ovary pathway. Notably, few direct downstream targets have been identified. We report that Wnt/β-catenin signaling directly stimulates *Irx3* and *Irx5* transcription in the developing ovary. Using *in silico* analysis of ATAC- and ChIP-Seq databases in conjunction with gonad explant transfection assays, we identified TCF/LEF binding sequences within two distal enhancers of the *IrxB* locus that promote β-catenin-responsive ovary expression. Meanwhile, *Irx3* and *Irx5* transcription is suppressed within the developing testis by the presence of H3K27me3 on these same sites. Thus, we resolved sexually dimorphic regulation of *Irx3* and *Irx5* via epigenetic and β-catenin transcriptional control where their ovarian presence promotes oocyte and follicle survival vital for future ovarian health.

Introduction

Early in development, the bipotential mammalian gonad can transform into a testis or an ovary depending on the activation or repression of signaling cascades in the somatic cell lineage (reviewed in (Svingen and Koopman, 2013)). In the ovary, the canonical Wnt4/Rspo1/β-catenin pathway plays a crucial role for proper differentiation and development (reviewed in (Nicol and Yao, 2014)). In XX mouse embryos, knockouts of *Wnt4* (Vainio et al., 1999, Jeays-Ward et al., 2004), *Rspo1* (Chassot et al., 2008, Tomizuka et al., 2008) or somatic cell loss of the downstream mediator, β-catenin, (Manuylov et al., 2008, Liu et al., 2009) results in a partial ovary to testis sex reversal and subsequent loss of 90% of the germ cell population by birth. Conversely, stabilization of β-catenin in the somatic cell population of the XY gonad leads to male-to-female sex reversal, suggesting that β-catenin is a crucial regulator of the sex identity of the somatic cell lineage (Maatouk et al., 2008). Multiple ovarian factors are thought to be regulated by β-catenin and its cognate DNA binding partners TCF/LEF, but a direct relationship in the ovary has yet to be elucidated.

Previously, we reported that two Iroquois homeobox transcription factors *Irx3* and *Irx5* are expressed in the ovary beginning shortly after sex differentiation. Each exhibits a dynamic profile during the course of germline nest establishment and breakdown through primordial follicle formation suggesting they play important roles in ovarian development (Kim et al., 2011, Fu et al., 2018). Iroquois factors are highly conserved factors that are known for their roles in patterning and embryogenesis, along with organization of the spinal cord, limb, bone, and heart (Bruneau et al., 2001, Diez del Corral et al., 1999, Gómez-Skarmeta et al., 2001, Gómez-Skarmeta and Modolell, 2002, Lovrics et al., 2014). Developmental regulation of these factors within these systems is context-specific as a number of signaling pathways have been described. Recently, we showed that null mutation of both *Irx3* and *Irx5* resulted in improper somatic-germ cell connections within follicles, which culminated in oocyte death (Fu et al., 2018). Notably, it was previously reported that the *Wnt4* knockout mouse also exhibited physical gaps between germ and somatic cells within follicles (Vainio et al., 1999), suggesting that Wnt and Iroquois factors may lie in the same pathway. *Irx3* and *Irx5* expression have been attributed to the canonical Wnt

signaling pathway in other tissues including the developing mouse ovary (Naillat et al., 2010a, Naillat et al., 2015), but a direct link to β-catenin/TCF/LEF transcriptional regulation has not been made.

Based on results from our and other studies, we hypothesized that *Irx3* and *Irx5* are direct transcriptional targets of the canonical Wnt/β-catenin pathway in the developing ovary. We detected no sex-specific regulatory activity within the proximal promoter regions using *ex vivo* gonad transfection assays. Instead, we uncovered two distant regulatory sequences within the *IrxB* locus that promote sexually dimorphic expression during critical stages of gonad differentiation. Herein, we report that active histone marks work together with β-catenin/TCF/LEF to bind and activate at least two enhancer regions within the *IrxB* locus to stimulate *Irx3* and *Irx5* transcription in the ovary. Meanwhile, these same sites were enriched for repressor H3K27me3 chromatin marks that actively repressed their transcription in developing testes. Together, these findings increase our perspective of the complex networks that are in place to ensure appropriate sex differentiation of gonads that include cooperation between epigenetic marks and transcription factors on promoter and distant regulatory sequences. In addition, this report uncovers mechanisms by which bipotential regulation can be achieved on the *IrxB* locus. These data provide a foundation for new discoveries of mechanisms by which canonical Wnt and other regulatory pathways work together to promote IRX3 and IRX5 function in a spatiotemporal manner within the developing ovary and during organogenesis of other systems including the heart, limb, bone and spinal cord.

Results

β-catenin activity correlates with *Irx3* and *Irx5* expression

Wnt4/Rspo1/β-catenin regulated transcription plays an essential role in ovarian development in somatic cells during sex differentiation. Our lab previously reported that *Irx3* and *Irx5* expression increased upon the onset of sex differentiation in the ovary (Fu et al., 2018) and these factors have been linked to canonical Wnt/β-catenin signaling in other tissues (Janssens et al., 2010, Naillat et al., 2010a, Naillat et al., 2015). Therefore, we hypothesized that canonical β-catenin regulates *Irx3* and

Irx5 in the somatic cells of the ovary at this time. To test this hypothesis, *ex vivo* and *in vivo* approaches were used to manipulate β-catenin activity to cause loss and gain-of-function in the developing ovary and testis, respectively. Embryonic day 11.5 (E11.5) wild-type ovaries were dissected and then cultured for 24 hours with two different dosages of iCRT14, a small molecule that inhibits the interaction between β-catenin and TCF/LEF family members to block β-catenin mediated gene transcription (**Fig. 1A)** (Yan et al., 2017, Gonsalves et al., 2011). As expected, treatment did not change the expression of *Rps29*, a ribosomal protein used as a negative control but inhibited β-catenin-responsive transcription in a dose-responsive manner. The 50μM dose decreased expression of known β-catenin target genes *Axin2* (77% decrease) and *Fst* (87% decrease) and caused a significant decrease in *Irx3* (73% decrease) and *Irx5* (76% decrease) transcripts (**Fig. 1B)**. Next, we evaluated *Irx3* and *Irx5* transcript accumulation in embryonic ovaries lacking somatic cell β-catenin activity that were generated by crossing *Sf1*Cre to *Ctnnb1*$^{F/F}$ mice (**Fig. S1**). *Rps29* transcripts from E14.5 control (*Sf1*Cre; *Ctnnb1*$^{F/+}$) and mutant (*Sf1Cre; Ctnnb1*$^{F/F}$) ovaries were not changed while *Axin2* and *Fst* were significantly decreased in mutant ovaries (76% and 96% decreased, respectively). In support of the *ex vivo* culture findings, *Irx3* and *Irx5* transcripts were also significantly decreased (65 and 60% decreased, respectively) in the mutant ovaries compared to the controls (**Fig. 1C)**. Together, *ex vivo* and *in vivo* results showed that the loss of β-catenin and its transcriptional activity in the developing ovary significantly diminished *Irx3* and *Irx5* expression.

Canonical Wnt/β-catenin is actively repressed in the developing testis (Kim et al., 2006, Uhlenhaut et al., 2009). Indeed, it has been shown that stabilization of β-catenin within the somatic cell population was sufficient to cause male-to-female sex reversal (Maatouk et al., 2008). Therefore, we evaluated whether β-catenin stabilization in the developing testis influenced *Irx3* and *Irx5* expression. Wild-type E11.5 testes were cultured *ex vivo* for 24 hours with Lithium Chloride (LiCl) to stabilize β-catenin (**Fig. 1A)**. Results from treated testes showed no change for *Rps29* and significantly increased expression of positive controls *Axin2* (4 fold) and *Fst* (10 fold). *Irx3* and *Irx5* transcripts also increased 9- and 5-fold, respectively,

compared to vehicle control (**Fig. 1D**). Previously it was reported that stabilized β-catenin activity in somatic cells of developing testes from *Sf1*Cre;*Ctnnb1*$^{\Delta ex3/+}$ (Harada et al., 1999) embryos caused sex reversal (Maatouk et al., 2008). Transcripts from control (No Cre;*Ctnnb1*$^{\Delta ex3/+}$) and mutant (*Sf1*Cre;*Ctnnb1*$^{\Delta ex3/+}$) testes (**Fig. S1**) at E14.5 displayed no significant change in *Rps29* transcript levels but exhibited significantly increased expression of *Axin2* (11 fold), *Fst* (7 fold), *Irx3* (16 fold), and *Irx5* (20 fold) (**Fig. 1E**) *Bmp2* was also used to test for Wnt/β-catenin specificity due to its role as a pro-ovarian gene that is not regulated by Wnt signaling.

Later in ovarian development, upon germline nest breakdown, *Irx3* expression expands to include both somatic cells and oocytes (Fu et al., 2018). β-catenin is also present in oocytes at this stage as shown by our immunohistochemistry results from ovaries at E14.5 and P7 and supported by previous reports (**Fig. S1, S2**) (Yan et al., 2019, Bothun and Woods, 2019, Kumar et al., 2016, Usongo et al., 2012, Chassot et al., 2011, Jameson et al., 2012). To test whether β-catenin activity regulates expression of *Irx3* within oocytes post germline nest breakdown, we targeted loss of *Ctnnb1* in oocytes using *Figla*Cre (Lin et al., 2014) and evaluated ovaries at P0 and P7 . Germ-cell specific loss of β-catenin using *Figla*Cre was confirmed (**Fig. S2A**); however, immunohistochemistry analysis indicated no obvious change in IRX3 within oocytes of mutant compared to control mice (**Fig. S2B**). Altogether these data suggest that canonical β-catenin transcriptional activity promotes *Irx3* and *Irx5* expression within somatic cells of the germline nest but does not regulate their transcription within oocytes upon their appearance during germline nest breakdown.

β-catenin responsive enhancer sites are present within the *IrxB* locus

Irx3 and *Irx5* are on opposing strands of DNA located 550kb apart within the *IrxB* cluster on chromosome 8 in the mouse (Cavodeassi et al., 2001, Peters et al., 2000). Given their proximity, we set out to identify accessible regions of chromatin within the *IrxB* locus. Previously, we performed DNaseI- and ATAC-seq on XY and XX somatic cell populations sorted from embryonic gonads at E10.5 (pre-sex determination) and E13.5 (post-sex determination) (Maatouk et al., 2017, Garcia-Moreno et al., 2019a). These datasets were used to interrogate chromosome 8 spanning 600kb on either

side of the *Irx3* transcription start site (tss) to search for areas of open chromatin that also included the consensus motif for β-catenin binding partners TCF/LEF (TCAAAG) (van de Wetering et al., 1997). Those sites that were used for further evaluation included those that were either resolved (R) by- or derived *de novo* (D) by E13.5 in the ovary (Garcia-Moreno et al., 2019a). Five sites of interest were identified and named based on their distances from the *Irx3* tss: +205kb, +86kb, -305kb (A,B), and -580kb (**see boxed peaks in Fig. 2**). The site at -305kb contained two separate TCF/LEF binding motifs, labeled 'A' and 'B'; all others harbored a single consensus element. A map detailing the approximate location of each site relative to *Irx3* and *Irx5* is outlined in **Fig. 2**.

To evaluate these open chromatin sites, we harvested ovaries and testes from E13.5-14.5 embryos to perform chromatin immunoprecipitation (ChIP) qPCR using antibodies for H3K27ac to mark active enhancer sites, and TCF7L2 to identify TCF/LEF binding sites relevant to the developing ovary. Of TCF/LEF factors, TCF7L2 was chosen for the following reasons: robust ChIP-seq data are available on the ENCODE database, microarray data indicating TCF7L2 is expressed predominantly in the somatic cells of the gonad (Jameson et al., 2012), and the GUDMAP database showed that TCF7L2 expression was detected in the ovary via *in situ* hybridization, whereas other TCF/LEF factors were negative (Harding et al., 2011, McMahon et al., 2008). For each replicate, whole gonad ChIP was first validated by showing RNA Polymerase II enrichment at the GAPDH promoter and TCF7L2 presence at a known β-catenin/TCF complex target, the SP5 promoter (Kennedy et al., 2016) in ovaries and testes (**Fig. S3**). TCF7L2 and H3K27ac are present in other cells besides pre-granulosa cells; therefore, we anticipated variability in ChIP-PCR data from replicates sourced from whole gonad tissue. Despite this potential barrier, our ChIP-PCR results showed substantial enrichment of H3K27ac and TCF7L2 binding on putative enhancer sequences in ovary (XX) compared to testis (XY) tissue (**Fig. 3**). Combined evaluation of H3K27ac and TCF7L2 results from ovary tissue suggest that β-catenin/TCF/LEF transcription factors bind and act on enhancer sequences at the +86kb (H3K27ac 20.1-fold; TCF7L2 2.2-fold enrichment) and -580kb (H3K27ac 11.1-fold; TCF7L2 2.7-fold

enrichment) sites to regulate *Irx3* and *Irx5* expression within developing ovaries. These results also suggest the potential for sex-specific regulation.

Constitutively active β-catenin defines the +86kb and -580kb sites as Wnt responsive enhancers in the *IrxB* locus

To test β-catenin responsive enhancer activity, each potential regulatory site was cloned into a luciferase reporter vector containing a minimal E1b promoter (Huang et al., 2006). In addition, each reporter vector was altered to include a single point mutation of the TCF/LEF binding motif (**T**CAAAG to **C**CAAAG), which is the same mutation that differentiates the TOPflash (active) versus FOPflash (inactive) β-catenin reporter plasmids (Korinek et al., 1997) (**Table S1**). Reporter plasmids were transfected into HEK293 cells along with a constitutively active β-catenin expression vector, CMV-S37A (Jordan et al., 2003). Specific β-catenin activity of the CMV-S37A expression vector was confirmed using co-transfection with positive and negative control reporter vectors, TOPflash and FOPflash, respectively (**Fig. S4**). Among all reporter vectors including +250kb, +86kb, -305kb (A, B), and -580kb, only the +86kb and -580kb plasmids exhibited a significant increase in reporter activity that was specific to the putative TCF/LEF binding site. Of note, the larger plasmid containing wild type -305ABkb sequences, which includes A and B TCF/LEF binding sites, was not responsive to CMV-S37A, and the double mutation of (A) and (B) had no effect (**Fig. 4A**). To test whether the +86kb and -580kb DNA enhancers (together equals 209bp) could stimulate promoter activity, both were cloned into the pGL3 basic luciferase reporter in front of 2,080bp of the mouse *Irx3* promoter (+86kb;-580kb;-1634/+446bp m*Irx3* pGL3). Constitutively active CMV-S37A cotransfected with the enhancer plus promoter reporter stimulated a 3 fold increase in activity compared to promoter alone. In addition, single base pair point mutations of the TCF/LEF binding site in each enhancer sequence completely disrupted enhancer activity (**Fig. 4B**). Together, these data suggest that the +86kb and -580kb enhancer sequences confer β-catenin specific regulatory activity within the context of the *Irx3* promoter.

+86kb and -580kb enhancers promote β-catenin specific activity in transfected fetal ovaries

Based on ovary-specific expression of *Irx3*, we reasoned that sequences within the *Irx3* promoter would confer ovary-specific expression. To test this hypothesis, three different sized segments of the mouse *Irx3* promoter (-351/+446bp, -603/+446bp, and -1634/+446bp) were cloned into a luciferase reporter plasmid and transfected into ovaries and testes from E13.5-14.5 embryos (**Fig. 5A**). While reporter activity increased along with longer promoter sequences, none of the promoters exhibited a significant difference when testis and ovary reporter activities were compared (**Fig. 5B**). Next, we tested whether β-catenin specific activity within the +86kb and -580kb enhancer sequences would promote ovary specific expression. Both enhancers and their mutated counterparts were cloned in front of the most active promoter (-1634/+446bp mIrx3pGL3) reporter vector and transfected into E14.5 gonads. While the enhancer plus m*Irx3* promoter was equally expressed in both ovary and testes, only ovary expression was disrupted upon single basepair point mutations of the TCF/LEF binding sites (60% decrease from wild type enhancers) (**Fig. 5C**). Based on these results we conclude that the +86kb and -580kb enhancer sequences promote β-catenin responsive activity only within the ovary.

+86kb and -580kb regions in the testis are enriched for H3K27me3

Plasmid vectors containing the enhancer sequences linked to the m*Irx3* promoter did not confer ovary versus testis specific reporter activity as expected; however, one limitation to this analysis is that plasmid reporter vectors lack epigenetic decorations that may have a profound impact on enhancer and/or promoter activity. Thus, we hypothesized that repressor histones suppress the +86kb and -580kb enhancer sequences within the developing testis. To test this hypothesis, we performed ChIP-Seq for the repressive histone modification H3K27me3 on FACS-purified XX and XY supporting cells from E13.5 gonads of *TESMS-CFP* (Gonen et al., 2018) and *Sox9-CFP* (Sekido and Lovell-Badge, 2008) transgenic mice, which fluorescently label granulosa (ovary) and Sertoli (testis) cells respectively. Each ChIP-seq experiment was performed on two biological replicates containing pooled cells from multiple gonads. To maintain consistency, we performed ChIP-seq on the same somatic cell

populations used for ATAC-seq (**Fig. 2**). To validate our datasets, we compared our results to previously published H3K27me3 ChIP-seq (performed on the same somatic populations) and found high correlation amongst all 4 biological replicates (**Fig 6A**). ChIP-seq data had previously been validated on promoters from genes known to drive sex determination and differentiation (Garcia-Moreno et al., 2019b). Results from ovary and testis H3K27me3 ChIP-seq are presented as peaks from individual replicates and include a solid horizontal bar above each set to illustrate the statistically positive sites as determined by HOMER analysis. Black vertical bars are included above these sites to illustrate positive ATAC-seq data. Results within the *Irx3/5* locus show that H3K27me3 marks are enriched at each of the four selected sites in the Sertoli cells but are absent in granulosa cells. In contrast, ATAC-seq peaks are stronger in granulosa cells as compared to Sertoli cells (**Fig. 6A**). To illustrate the dynamic nature of epigenetic regulation that occurs during sex determination, we present a magnified view of the select sequences with a representative H3K27me3- and ATAC-seq replicate at E10.5 (pre-sex determination) and E13.5 (post-sex determination) in XX and XY supporting cells (**Fig. 6B**). Stage dependent epigenetic control is evident at each enhancer site. At +205kb, chromatin, which is initially accessible pre-sex determination, remains open in granulosa cells, whereas it transitions to a repressed and closed state in Sertoli cells at E13.5. At +86kb, chromatin is initially open in both XX and XY at E10.5. At E13.5, accessibility increases and H3K27me3 decreases in granulosa cells, whereas H3K27me3 levels increase in the Sertoli cells. Finally, closed chromatin at -306kb and -580kb, becomes accessible in granulosa cells at E13.5, whereas this sites accumulate H3K27me3 in Sertoli cells.

Taken together, our data uncovers two specific enhancers within the *IrxB* locus that confer ovary versus testis specific promoter activity. In the ovary, canonical β-catenin activity cooperates with active epigenetic marks on open chromatin to stimulate the +86kb and -580kb enhancers while expression is silenced in the testis due to the combined effects of histone methylation repression and the lack of functional β-catenin activity.

Discussion

Canonical Wnt/β-catenin signaling has been reported to promote *Irx3* and *Irx5* expression in the ovary (Naillat et al., 2010b, Naillat et al., 2015) and other tissues such as the brain (Braun et al., 2003), lung (Bell et al., 2008), neural axis (Janssens et al., 2010), kidney (Holmquist Mengelbier et al., 2019), and in colon cancer (Hovanes et al., 2001), but evidence for direct trans-acting regulation via DNA binding partners has not been elucidated. Here we used *in vitro, ex vivo*, and *in vivo* approaches to provide a direct link between canonical Wnt/β-catenin signaling and *Irx3* and *Irx5* expression within the somatic cell population of the developing ovary. In addition, we previously showed that both Iroquois factors emerge in germ cells in late stages of ovarian development (Fu et al., 2018), but here we report that their regulation in this cell type is independent of β-catenin. Based on these data, we developed a model to describe regulation of *Irx3* and *Irx5* expression within the somatic cell population (**Fig. 7**). We uncovered two enhancer sequences that, although distant from the transcription start site, they provide the focus for regulation within the ovary and testis. Our data indicate that chromatin enhancer marks work in conjunction with β-catenin/TCF/LEF at these sites to stimulate the *IrxB* locus in the ovary, while the absence of activated β-catenin in somatic cells along with repressive histone marks enriched at these same sites functionally antagonize expression of *Irx3* and *Irx5* in the testis. Together, these findings highlight interactions between signaling pathways and epigenetic marks that regulate *Irx3* and *Irx5* to ensure appropriate expression based on time, sex, and cellular environments within developing gonads.

We examined ~1200kb of chromosome 8, which included the *IrxB* and *Fto* loci, for female-specific open chromatin sites that could also mediate canonical β-catenin regulation within somatic cells after sex differentiation. Altogether, our DNAseI-Seq (Maatouk et al., 2017) and ATAC-Seq (Garcia-Moreno et al., 2019a) data, along with results from ENCODE ChIP-Seq derived TCF/LEF enrichment in human cell lines (Consortium, 2012) illuminated five putative sites that met these criteria. Notably, none were identified within the proximal promoters of either *Irx3* or *Irx5*. One limitation to this study is that only perfect matches to the TCF/LEF binding domains

were explored. HMG box transcription factors, such as TCF/LEF, can also bind to DNA motifs that do not match the perfect consensus sequence; therefore, all potential binding regions were not explored. There were also several sex-specific sites of open chromatin within the *IrxB* locus that were not considered. Regarding the nucleosome depleted regions that were evaluated in this study, JASPAR database interrogations uncovered a variety of other putative binding sites (Khan et al., 2018). These *in silico* analyses did not distinguish any common suite of transcription factor binding sites within either the resolved or *de novo* open chromatin regions. In particular, the two sites that we identified as the most promising β-catenin-responsive enhancers in the ovary, +86kb and -580kb, were characterized as resolved and *de novo* sites, respectively. Besides TCF7L2, the +86kb site harbors sequences that also bind CTCF, p300, and YY1, factors that are important for facilitating higher order chromatin structures (Ghirlando and Felsenfeld, 2016, Chan and La Thangue, 2001, Deng et al., 2010). These findings, in combination with the significant distance between enhancer sites and our results that show that 20-40% of *Irx3* and *Irx5* transcripts remain after elimination of β-catenin suggest that chromatin encompassing the *IrxB* locus loops and undergoes extensive remodeling in response to sex-specific signals and developmental time.

An important goal of our study was to determine the relevance of putative enhancer sequences in promoting ovary-specific expression of *Irx3* and *Irx5*. To that end, we combined traditional cell-based transfection assays with our previously described microinjection and electroporation technique to transfect reporter plasmids into embryonic gonads (Gao et al., 2011) with a specific focus on the mouse *Irx3* promoter (m*Irx3*-pGL3). We were surprised to find that the enhancer/m*Irx3* promoter reporters were equally active in ovaries and testes. There are a number of potential reasons for this result. For example, it is recognized that reporter plasmid DNA transfection assays are used to focus attention to specific sequences, which are not in their normal context and therefore, must be interpreted as such. In addition, plasmid DNA is devoid of epigenetic information which has important implications on regulation. Indeed, our H3K27me3-Seq data show substantial enrichment at the proximal promoters of *Irx3* and *Irx5* only in XY cells (**Fig. S5**). Further, our results showed that the response to mutation of the canonical TCF/LEF binding site was not

present in transfected testes, but was sensitive in cell and ovary transfection, both of which are β-catenin-responsive environments. Additional JASPAR analysis of the enhancer and promoter sequences uncovered several putative binding sites including SOX, GATA, EZH2, CEBP, and SP1 factors among others. Together, these findings support the hypothesis that ovary-specific regulation for *Irx3* and *Irx5* is linked to canonical β-catenin signaling and opens the door for other means of regulation in the context of the loss of epigenetic marks that might explain high levels of testis reporter activity.

Because we expected reporter activity to be lower in transfected testes compared to ovaries, we evaluated the enhancer sites for histone repressor marks and found H3K27me3 marks were specifically enriched at +86kb and -580kb enhancer sites in addition to the proximal promoters of *Irx3* and *Irx5* in somatic cells of testes, but not ovaries. Thus, taken together, we conclude that both +86kb and -560kb open sites are subject to changing epigenetic landscapes. In newly differentiated ovarian somatic cells, active β-catenin/TCF complexes accumulate on the *IrxB* locus to stimulate *Irx3* and *Irx5* transcription. In contrast, somatic cells that are destined for the testis phenotype lack β-catenin and instead, recruit epigenetic decorations consistent with transcriptional repression.

Irx3 and *Irx5* show dynamic ovary-specific expression profiles (Fu et al., 2018). Besides canonical Wnt/β-catenin signaling, *Irx3* has also been shown to be controlled by other pathways including TGFβ (Cavodeassi et al., 2001, JL, 1998), SHH (Briscoe et al., 2000, Kobayashi et al., 2002), FGF (Kobayashi et al., 2002), and Retinoic acid (Sirbu et al., 2005). Notably, many of these ligands have been established as sex-specific signals that also depend on a cadre of active transcription factors and epigenetic marks within the somatic cell population during the sex differentiation window (Garcia-Moreno et al., 2018, Garcia-Moreno et al., 2019a, Katoh-Fukui et al., 2012, Hiramatsu et al., 2009, Morais da Silva et al., 1996). But important questions remain: who comes first and who regulates whom? An interesting conundrum related to this question was illustrated in the evolving story of CBX2 regulation of *Sry*. Originally, it was proposed that CBX2, a subunit of the

canonical Polycomb Repressive Complex 1 (PRC1) acted as a direct activator of *Sry* (Katoh-Fukui et al., 2012). New studies have since refined this discovery and now show that within the developing testis, CBX2 and PRC1 establish repressor H3K27me3 marks to extinguish the rising profile of ovary pathway genes, which allows for accumulation of *Sry* (Garcia-Moreno et al., 2019b). Other chromatin modifiers, including GLP-G9a/JMJD1 and CBP/p300 contribute to *Sry* expression by modulating H3K9Me2 repressor and H3K27ac marks (Kuroki et al., 2013, Kuroki et al., 2017, Carré et al., 2018). These new data illustrate how epigenetic writers and readers can play a critical role in sex determination and differentiation. Important insight can also be learned from species where sex determination is influenced by both genes and environmental cues. Indeed, there is a growing field in developmental epigenetics that increasingly recognizes that environmental cues are translated into specific sex phenotypes via epigenetic manipulations of sex determining genes (Navarro-Martín et al., 2011, Matsumoto et al., 2013, Parrott et al., 2014, Piferrer, 2013). Ultimately, plastic epigenetic marks provide flexibility and a means to preserve survival of sexually reproductive species.

The results of this study highlight the importance of transcription factor binding and local epigenetic landscape in illuminating cell and sex-defining fates during gonadogenesis. Distant enhancer sites have long been implicated in gene control in the gonad and new technologies are improving our capacity to identify and validate their importance (Sekido and Lovell-Badge, 2008, Gonen et al., 2018, Gonen et al., 2017). Here, we describe two distal enhancer sites on the *IrxB* locus that are actively repressed in developing testes while at the same time, are engaged with active chromatin marks and β-catenin/TCF to stimulate *Irx3* and *Irx5* expression within the developing ovary. Thus, *Irx3* and *Irx5* are bonafide downstream targets of Wnt/Rspo1/β-catenin that together, are critical mediators of ovary development and oocyte survival. These findings allow us to begin to unravel the means by which specific cell environments control *Irx3* and *Irx5* expression within the fetal ovary. We suggest that these same principles could be applied to the developing brain, spinal cord, lung, kidney, or to abnormal cellular activity in Iroquois-positive cancers.

Methods & Materials

Animals

Mouse strains included CD1 outbred mice (Crl:CD1(ICR), Charles River, MA); *Sf1*Cre mice (C57BL/6), originally obtained from the Keith Parker Lab (Bingham et al., 2006); *Ctnnb1* conditional loss-of-function (LOF) mice (B6.129-*Ctnnb1*^{tm2Kem}/KnwJ, Jackson Labs); and *Ctnnb1* conditional gain-of-function (GOF) mice (C57BL/6; *β-cat*$^{fl.ex3}$), obtained from Dr. Makoto Mark Taketo, Kyoto University, Kyoto, Japan (Harada et al., 1999), *Sox9-CFP* (Sekido and Lovell-Badge, 2008), and *TESMS-CFP* (Gonen et al., 2018). Timed mating was identified by the presence of a vaginal plug, which was designated as embryonic day 0.5 (E0.5). Animals were dissected at the appropriate time and genomic DNA was isolated from tails or ear notches and subjected to PCR using gene specific primers: *Sf1*Cre: 5′-GAGTGAACGAACCTGGTCGAAATCAGTGCG-3′ and 5′-GCATTACCGGTCGATGCAACGAGTGATGAG-3′; *Ctnnb1* wild-type and floxed (LOF) allele 5′-AAGGTAGAGTG ATGAAAGTTGTT-3′ and 5′-CACCATTGTCCTCTGTCTATTC -3′; *Ctnnb1* wild-type and *β-cat*$^{fl.ex3}$ (GOF) allele 5’-GCTGCGTGGACAATGGCTACTCAA-3’ and 5’-GCCATGTCCAACTCCATCAGGTCA-3’. In the case where sex could not be determined visually, PCR for SRY was performed: 5’-TGCAGCTCTACTCCAGTCTTG-3’ and 5’-GATCTTGATTTTTAGTGTTC-3’.

Animal housing and all procedures described were reviewed and approved by the Institutional Animal Care and Use Committee at the University of Wisconsin-Madison and were performed in accordance with the National Institute of Health Guiding Principles for the Care and Use of Laboratory Animals. Mice were housed in disposable, ventilated cages (Innovive, San Diego, CA). Rooms were maintained at 22 ±2 degrees Celsius and 30–70% humidity on a 12 hour light/dark cycle.

Organ culture using the droplet method

Gonad cultures were performed using a modified version of previously described protocols (Martineau et al., 1997, Maatouk et al., 2008). Briefly, E11.5 gonad/mesonephros complexes were cultured at 37°C with 5%CO_2/95% air in ~20µl

droplet of culture media (DMEM F-12 (Fisher, SH3002301)) supplemented with 10% fetal bovine serum (Fisher, SH3091003) and 1% Penicillin-Streptomycin (Fisher, ICN1670249). Sex of the gonads was determined by genotyping PCR for SRY (see above). Gonad/mesonephros complexes were placed in round droplets of media on an inverted lid of a 100mm Petri dish within a humidified chamber. Gonads (XX and XY) were cultured in a droplet supplemented with either vehicle control, the indicated concentrations of iCRT14 (XX gonads, Sigma SML0203), or LiCl (XY gonads, Fisher L121-100) for 24 hours, rinsed with PBS and then harvested for RNA extraction and qPCR analysis.

RNA Extraction and qPCR

RNA was extracted using Trizol (Invitrogen, ca#: 15596026) according to the manufacturer's instructions and quantified using a NanoDrop 2000. 500ng RNA from each sample was used for First-Strand cDNA synthesis by SuperScriptII-RT (Invitrogen, AM9515). cDNA was diluted 1:5 and then 2 µl was added to 5 µl SYBR green PCR mixture (Applied Biosystems), 2.4 µl water, and 1.25 pmol primer mix. PCR reactions were carried out using the ABI Prism 7000 Sequence Detection System (Applied Biosystems). RNA transcripts were quantified using the ΔΔCt method (Livak and Schmittgen, 2001). Briefly, to control for overall gene expression in each time point, the average cycle threshold (aveCt) for 36B4 was subtracted from the aveCt value for each gene to generate ΔCt. Next, ΔCt for each gene was compared to ΔCt of that same gene for the mutant genotype (e.g. $\Delta Ct\ Irx3_{female\ control} - \Delta Ct\ Irx3_{female\ mutant}$), to generate ΔΔCt. Finally, fold change was calculated as 2 to the −ΔΔCt power ($2^{-\Delta\Delta Ct}$). Primers are listed in **Supplementary Table S2**.

DNase-I seq, ATAC-seq cluster analysis, and ChIP-seq cluster analysis

DNAse-I, ATAC-seq, and H3K27me3 data were mined from these studies: (Maatouk et al., 2017, Garcia-Moreno et al., 2019b, Garcia-Moreno et al., 2019a). These data were analyzed for open chromatin regions within 600kb on either side of the *Irx3* transcription start site (tss) of chromosome 8 in the mouse. Open chromatin regions that were specific to the granulosa cells after sex determination (E13.5) were explored for TCF/LEF binding motifs using the JASPAR database

(jaspar.genereg.net). The sequences containing the highest scores for binding potential were chosen for further investigation.

Chromatin Immunoprecipitation followed by qPCR

E13.5-E14.5 CD1 ovaries and testes without mesonephros were harvested, snap frozen, and stored at -80°C. 100-150 pairs of snap-frozen gonads were thawed and fixed in 1% formaldehyde for 15 min at room temperature with gentle shaking. The reaction was quenched with 160 µL of 1.25 M glycine for 5 min at room temp with gentle shaking. Samples were washed 2x with PBS and cOmplete™ protease inhibitor (CPI) tablets (Roche, Basel, Switzerland; catalog #04693116001) then resuspended in 400 µL RIPA lysis buffer + CPI tablets. Samples were homogenized with a pestle, then chromatin shearing was performed by lightly sonicating via probe-based sonication to fully lyse cells and the nuclear envelope followed by 1 minute incubation at 37°C using 1000 gel units of Micrococcal Nuclease (MNase) (New England Biolabs; catalog #M0247S). A separate 5µL sample was incubated with Proteinase K to validate efficient shearing of DNA (between 300 bp–900 bp). The MNase reaction was stopped with 1.25 µmol EGTA. Debris was removed by centrifugation at 15,000 g for 10 m at 4 °C and then 100 µL of each lysate was diluted in 200 µL IP buffer (PBS + 0.05% Triton X-100) and incubated overnight with 2 µg of antibody. After overnight antibody incubation, 25 µL of Dynabeads protein G magnetic beads (Life Technologies; catalog #10004D) was added and mixed for 2 hours at 4 °C with gentle rocking. Samples were washed sequentially with 500 µL Low Salt, 500 µL High Salt, and 500 µL TE Buffers, then resuspended in Digestion Buffer (50 mM Tris, 10 mM EDTA, 0.5% SDS, pH 8.0) + Proteinase K for 2 hours at 62 °C. DNA was isolated via ethanol precipitation. qPCR analysis was performed to quantify relative amounts of DNA enrichment; immunoprecipitated (IP) samples were normalized to input and IgG. Antibodies used: Anti-phospo RNA PolII (Ser2), clone 3 (Millipore MABE954), Normal Mouse IgG (Sigma, M8695), TCF4 (C4H811) (Cell Signaling Technology, #2569S), and Histone H3K27ac (Active Motif, Cat#39133).

Chormatin Immunoprecipitation followd by next-generation sequencing

ChIP-seq was performed and analyzed as in Garcia-Moreno et al., 2019b. Briefly, XX and XY supporting cells were FACS-purified from E13.5 XY *SOX9-CFP* gonads

and E13.5 XX *TESMS-CFP* gonads on the same day, and immediately processed for ChIP-seq. ChIP-seq was performed with no modifications as in (Van Galen et al., 2016) on 2 biological replicates, each containing ~150K FACS-purified supporting cells from pooled gonads. 400K *Drosophila* S2 cells were added per IP as carrier chromatin. ChIP-seq was performed using 3μl of H3 antibody (Active Motif #39763) (used as input), or 5μl H3K27me3 antibody (CST#9733S).

Sequence alignment to the mm9 mouse genome was performed using Bowtie. H3 ChIP-seq was used as input. To identify regions significantly enriched for H3K27me3 compared to flanking regions (peaks), HOMER was used for each independent replicate using the findPeaks function and settings "—style histone" and "-C 0", with a size of 5000. BigWig files were created using bedGraphToBigWig for visualization on the UCSC genome browser.

Plasmid Constructs

Luciferase reporters were generated from mouse genomic sequences of the enhancers at +205kb, +86kb, -305kb, and -580kb from the *Irx3* tss specific to the region containing the TCF/LEF binding motif via PCR with the addition of the KpnI and XhoI restriction enzyme sequences (**Supplementary Table S1**). Each sequence was digested and inserted into the pGL3 basic vector containing a minimal E1b promoter (Huang et al., 2006) digested at the KpnI and XhoI sites. The QuikChangeII site-directed mutagenesis kit was used to make a single base pair mutation for each TCF/LEF binding site as directed in the manufacturer's protocol (Stratagene) (**Supplementary Table S1**). The mouse *Irx3* promoter construct was generated from mouse genomic sequence using primers specific to 1634bp upstream and 446bp downstream of the *Irx3* tss and placed into the pGL3 basic vector. The +86kb and -580kb sequences were inserted in front of the mouse *Irx3* promoter using the NEBuilder HiFi DNA Assembly Cloning Kit according the manufacturer's instructions (New England BioLabs, E5520S). Each reporter construct was sequenced for accuracy after initial construction and proper mutation following mutagenesis (Sanger sequencing, UW Madison Biotech Center).

Plasmids containing promoter regions of *Irx3* were constructed via the Ensembl *Irx3* gene sequence and primer design software (Primer Designer version 1.01). PCR primers targeted the promoter region 5' of the *Irx3* tss. Genomic DNA was amplified, and inserts were blunt-end ligated into the pST-blue Accepter vector (Novagen). Sequencing was then performed (Keck Center, University of Illinois); the insert sequence was compared to the archived DNA sequence (NT_078586.1) and validated for accuracy.

Cell culture and Transient Transfection

80,000 HEK293 cells (purchased from ATCC®, catalog #CRL-1573, validated before shipment) were plated in 24 well plates (Thermo Scientific, catalog #12565163) for transfection assays. Plasmids were prepped using column based mini or midi prep kits (Qiagen, cat#27104, cat#12143) and quantified using a NanoDrop 2000. Cells were transfected using Lipofectamine 2000 (Invitrogen, cat#11668019) with plasmid DNA diluted in OPTI-MEM media (Fisher, cat#31985070) according to the manufacturer's instructions. Luciferase reporter vectors were transfected at 0.8µg/well along with 50ng/well co-expression vector CMV-EGFP (Addgene #11153) or CMV-S37A-β-catenin (Jordan et al., 2003) (kindly provided by Dr. Vincent Harley, Hudson Institute for Medical Research, Monash University, Melbourne, Australia) for normalization or treatment, respectively. The lipofectamine 2000 mixture was incubated with the cells for 16-18 hours followed by a media change. After 24 hours, the cells were lysed using 1X Passive lysis buffer and read using the Dual Luciferase Reporter Assay (Promega, E1910). Treatment groups were plated in triplicate and experiments were repeated at least three times. Luciferase values from the treatment group were normalized to the non-treatment group and also normalized to the empty vector control.

Gonad Injection and Electroporation

Transient transfection assays in urogenital ridge explant cultures were based on previously reported methods of the explant culture system (Jorgensen and Gao, 2005). The sex of the gonad tissue was determined by characteristic findings of a coelomic vessel and testicular cords in the male and the lack of these in the female. Urogenital ridges were harvested from embryos at E14.5 and injected with

approximately 0.5μL of a DNA cocktail containing 4 μg/μl pGL3, wild type +86kb/-580kb/mIrx3 promoter pGL3, or mutated +86kb/-580kb/mIrx3 promoter pGL3 plus 2 μg/μl SV40-Renilla luciferase in Dulbecco phosphate-buffered saline (PBS; Sigma D8537). An additional aliquot of 25 μl of sterile PBS was placed on the gonad for electroporation. Immediately thereafter, five square electrical pulses of 65 V, 50 msec each at 100-msec intervals, were delivered through platinum electrodes from an electroporator. After electroporation, urogenital ridges were placed back into the culture for 24 hours. Explant cultures were maintained at 37°C with 5% CO_2/95% air in 50 μl of Dulbecco minimal Eagle medium (DMEM) supplemented with 10% FBS (fetal bovine serum) and 1% Penicillin/Streptomycin. Transfected gonad explants were harvested in 50μl passive lysis buffer, snap frozen, subjected to three freeze-thaw cycles, and then processed for dual luciferase assays. Data were calculated by taking the ratio of luciferase to renilla expression with at least 3 biological replicates for each injected plasmid.

Statistics

Statistics between groups were carried out using a two-tailed t-test assuming unequal variances. Results were considered statistically significant if p-values were ≤ 0.05. One-way ANOVA Post-hoc Tukey was performed where appropriate.

Acknowledgements

Special thanks to all members of the Jorgensen lab for ideas and support throughout this work; in addition, Drs. John Svaren and Linda Schuler for extraordinary consultation. We are also extremely grateful for the technical support from Dr. Camila Lopez-Anido and Dr. John Svaren in our ChIP experiments. Also, thank you to Janelle Ryan and Dr. Vincent Harley for the CMV-S37A active β-catenin plasmid. We have an immense amount of gratitude to the cohort of undergraduates that helped with immunofluorescence, genotyping, and sectioning, especially Linda Wang, Ann Turcotte, and Rebekah Schroeder. In addition, thanks to the University of Wisconsin Biotron for the exemplary mouse husbandry help.

Dedicated to Danielle M. Maatouk, a wonderful colleague, scientist, and friend.

Competing Interests

No competing interests to declare.

Funding Support

This work was supported by the National Institutes of Health: R21HD48911, R01HD075079, and R01HD090660 to JSJ; R01HD090660-Reentry Supplement to AK; T32GM008688 to MLK; T32GM008061 to SAGM. In addition, this research was also supported in part by the Intramural Research Program of the National Institutes of Health at the National Institute of Environmental Health Sciences (NIH-ZIAES102965 to H.H-C.Y.).

References

BELL, S. M., SCHREINER, C. M., WERT, S. E., MUCENSKI, M. L., SCOTT, W. J. & WHITSETT, J. A. 2008. R-spondin 2 is required for normal laryngeal-tracheal, lung and limb morphogenesis. *Development (Cambridge, England),* 135**,** 1049-1058.

BINGHAM, N. C., VERMA-KURVARI, S., PARADA, L. F. & PARKER, K. L. 2006. Development of a steroidogenic factor 1/Cre transgenic mouse line. *Genesis (New York, N.Y. : 2000),* 44**,** 419-24.

BOTHUN, A. M. & WOODS, D. C. 2019. Dynamics of WNT signaling components in the human ovary from development to adulthood. *Histochem Cell Biol,* 151**,** 115-123.

BRAUN, M. M., ETHERIDGE, A., BERNARD, A., ROBERTSON, C. P. & ROELINK, H. 2003. Wnt signaling is required at distinct stages of development for the induction of the posterior forebrain. *Development (Cambridge, England),* 130**,** 5579-5587.

BRISCOE, J., PIERANI, A., JESSELL, T. M. & ERICSON, J. 2000. A homeodomain protein code specifies progenitor cell identity and neuronal fate in the ventral neural tube. *Cell,* 101**,** 435-45.

BRUNEAU, B. G., BAO, Z. Z., FATKIN, D., XAVIER-NETO, J., GEORGAKOPOULOS, D., MAGUIRE, C. T., BERUL, C. I., KASS, D. A., KUROSKI-DE BOLD, M. L., DE BOLD, A. J., CONNER, D. A., ROSENTHAL, N., CEPKO, C. L., SEIDMAN, C. E. & SEIDMAN, J. G. 2001. Cardiomyopathy in Irx4-deficient mice is preceded by abnormal ventricular gene expression. *Mol Cell Biol,* 21**,** 1730-6.

CARRÉ, G. A., SIGGERS, P., XIPOLITA, M., BRINDLE, P., LUTZ, B., WELLS, S. & GREENFIELD, A. 2018. Loss of p300 and CBP disrupts histone acetylation at the mouse Sry promoter and causes XY gonadal sex reversal. *Hum Mol Genet,* 27**,** 190-198.

CAVODEASSI, F., MODOLELL, J. & GÓMEZ-SKARMETA, J. L. 2001. The Iroquois family of genes: from body building to neural patterning. *Development,* 128**,** 2847-55.

CHAN, H. M. & LA THANGUE, N. B. 2001. p300/CBP proteins: HATs for transcriptional bridges and scaffolds. *J Cell Sci,* 114**,** 2363-73.

CHASSOT, A.-A., GREGOIRE, E. P., LAVERY, R., TAKETO, M. M., DE ROOIJ, D. G., ADAMS, I. R. & CHABOISSIER, M.-C. 2011. RSPO1/β-catenin signaling pathway regulates oogonia differentiation and entry into meiosis in the mouse fetal ovary. *PloS one,* 6**,** e25641-e25641.

CHASSOT, A. A., RANC, F., GREGOIRE, E. P., ROEPERS-GAJADIEN, H. L., TAKETO, M. M., CAMERINO, G., DE ROOIJ, D. G., SCHEDL, A. & CHABOISSIER, M. C. 2008. Activation of β-catenin signaling by Rspo1 controls differentiation of the mammalian ovary. *Human Molecular Genetics,* 17**,** 1264-1277.

CONSORTIUM, E. P. 2012. An integrated encyclopedia of DNA elements in the human genome. *Nature,* 489**,** 57-74.

DENG, Z., CAO, P., WAN, M. M. & SUI, G. 2010. Yin Yang 1: a multifaceted protein beyond a transcription factor. *Transcription,* 1**,** 81-4.

DIEZ DEL CORRAL, R., AROCA, P., G MEZ-SKARMETA, J. L., CAVODEASSI, F. & MODOLELL, J. 1999. The Iroquois homeodomain proteins are required to specify body wall identity in Drosophila. *Genes Dev,* 13**,** 1754-61.

FU, A., OBERHOLTZER, S. M., BAGHERI-FAM, S., RASTETTER, R. H., HOLDREITH, C., CACERES, V. L., JOHN, S. V., SHAW, S. A., KRENTZ, K. J., ZHANG, X., HUI, C. C., WILHELM, D. & JORGENSEN, J. S. 2018. Dynamic expression patterns of Irx3 and Irx5 during germline nest breakdown and primordial follicle formation promote follicle survival in mouse ovaries. *PLoS Genet,* 14**,** e1007488.

GAO, L., KIM, Y., KIM, B., LOFGREN, S. M., SCHULTZ-NORTON, J. R., NARDULLI, A. M., HECKERT, L. L. & JORGENSEN, J. S. 2011. Two regions within the proximal steroidogenic factor 1 promoter drive somatic cell-specific activity in developing gonads of the female mouse. *Biology of reproduction,* 84**,** 422-34.

GARCIA-MORENO, S. A., FUTTNER, C. R., SALAMONE, I. M., GONEN, N., LOVELL-BADGE, R. & MAATOUK, D. M. 2019a. Gonadal supporting cells acquire sex-specific chromatin landscapes during mammalian sex determination. *Dev Biol,* 446**,** 168-179.

GARCIA-MORENO, S. A., LIN, Y. T., FUTTNER, C. R., SALAMONE, I. M., CAPEL, B. & MAATOUK, D. M. 2019b. CBX2 is required to stabilize the testis pathway by repressing Wnt signaling. *PLoS Genet,* 15**,** e1007895.

GARCIA-MORENO, S. A., PLEBANEK, M. P. & CAPEL, B. 2018. Epigenetic regulation of male fate commitment from an initially bipotential system. *Mol Cell Endocrinol,* 468**,** 19-30.

GHIRLANDO, R. & FELSENFELD, G. 2016. CTCF: making the right connections. *Genes Dev,* 30**,** 881-91.

GÓMEZ-SKARMETA, J., DE LA CALLE-MUSTIENES, E. & MODOLELL, J. 2001. The Wnt-activated Xiro1 gene encodes a repressor that is essential for neural development and downregulates Bmp4. *Development,* 128**,** 551-60.

GÓMEZ-SKARMETA, J. L. & MODOLELL, J. 2002. Iroquois genes: genomic organization and function in vertebrate neural development. *Curr Opin Genet Dev,* 12**,** 403-8.

GONEN, N., FUTTNER, C. R., WOOD, S., GARCIA-MORENO, S. A., SALAMONE, I. M., SAMSON, S. C., SEKIDO, R., POULAT, F., MAATOUK, D. M. & LOVELL-BADGE, R. 2018. Sex reversal following deletion of a single distal enhancer of. *Science,* 360**,** 1469-1473.

GONEN, N., QUINN, A., O'NEILL, H. C., KOOPMAN, P. & LOVELL-BADGE, R. 2017. Normal Levels of Sox9 Expression in the Developing Mouse Testis Depend on the TES/TESCO Enhancer, but This Does Not Act Alone. *PLoS Genet,* 13**,** e1006520.

GONSALVES, F. C., KLEIN, K., CARSON, B. B., KATZ, S., EKAS, L. A., EVANS, S., NAGOURNEY, R., CARDOZO, T., BROWN, A. M. & DASGUPTA, R. 2011. An RNAi-based chemical genetic screen identifies three small-molecule inhibitors of the Wnt/wingless signaling pathway. *Proc Natl Acad Sci U S A,* 108**,** 5954-63.

HARADA, N., TAMAI, Y., ISHIKAWA, T., SAUER, B., TAKAKU, K., OSHIMA, M. & TAKETO, M. M. 1999. Intestinal polyposis in mice with a dominant stable mutation of the beta-catenin gene. *The EMBO journal,* 18**,** 5931-42.

HARDING, S. D., ARMIT, C., ARMSTRONG, J., BRENNAN, J., CHENG, Y., HAGGARTY, B., HOUGHTON, D., LLOYD-MACGILP, S., PI, X., ROOCHUN, Y., SHARGHI, M., TINDAL, C., MCMAHON, A. P., GOTTESMAN, B., LITTLE, M. H., GEORGAS, K., ARONOW, B. J., POTTER, S. S., BRUNSKILL, E. W., SOUTHARD-SMITH, E. M., MENDELSOHN, C., BALDOCK, R. A., DAVIES, J. A. & DAVIDSON, D. 2011. The GUDMAP database--an online resource for genitourinary research. *Development,* 138**,** 2845-53.

HIRAMATSU, R., MATOBA, S., KANAI-AZUMA, M., TSUNEKAWA, N., KATOH-FUKUI, Y., KUROHMARU, M., MOROHASHI, K., WILHELM, D., KOOPMAN, P. & KANAI, Y. 2009. A critical time window of Sry action in gonadal sex determination in mice. *Development,* 136**,** 129-38.

HOLMQUIST MENGELBIER, L., LINDELL-MUNTHER, S., YASUI, H., JANSSON, C., ESFANDYARI, J., KARLSSON, J., LAU, K., HUI, C. C., BEXELL, D., HOPYAN, S. & GISSELSSON, D. 2019. The Iroquois homeobox proteins IRX3 and IRX5 have distinct roles in Wilms tumour development and human nephrogenesis. *J Pathol,* 247**,** 86-98.

HOVANES, K., LI, T. W., MUNGUIA, J. E., TRUONG, T., MILOVANOVIC, T., LAWRENCE MARSH, J., HOLCOMBE, R. F. & WATERMAN, M. L. 2001. Beta-catenin-sensitive isoforms of lymphoid enhancer factor-1 are selectively expressed in colon cancer. *Nat Genet,* 28**,** 53-7.

HUANG, M., JIA, F. J., YAN, Y. C., GUO, L. H. & LI, Y. P. 2006. Transactivated minimal E1b promoter is capable of driving the expression of short hairpin RNA. *J Virol Methods,* 134**,** 48-54.

JAMESON, S. A., NATARAJAN, A., COOL, J., DEFALCO, T., MAATOUK, D. M., MORK, L., MUNGER, S. C. & CAPEL, B. 2012. Temporal transcriptional profiling of somatic and germ cells reveals biased lineage priming of sexual fate in the fetal mouse gonad. *PLoS Genet,* 8**,** e1002575.

JANSSENS, S., DENAYER, T., DEROO, T., VAN ROY, F. & VLEMINCKX, K. 2010. Direct control of Hoxd1 and Irx3 expression by Wnt/beta-catenin signaling during anteroposterior patterning of the neural axis in Xenopus. *The International journal of developmental biology,* 54**,** 1435-42.

JEAYS-WARD, K., DANDONNEAU, M. & SWAIN, A. 2004. Wnt4 is required for proper male as well as female sexual development. *Developmental biology,* 276**,** 431-40.

JL, G.-S. 1998. Xiro, a Xenopus homolog of the Drosophila Iroquois complex genes, controls development at the neural plate. *In:* A, G. (ed.). EMBO J.

JORDAN, B. K., SHEN, J. H., OLASO, R., INGRAHAM, H. A. & VILAIN, E. 2003. Wnt4 overexpression disrupts normal testicular vasculature and inhibits testosterone synthesis by repressing steroidogenic factor 1/beta-catenin synergy. *Proc Natl Acad Sci U S A,* 100**,** 10866-71.

JORGENSEN, J. S. & GAO, L. 2005. Irx3 is differentially up-regulated in female gonads during sex determination. *Gene expression patterns : GEP,* 5**,** 756-62.

KATOH-FUKUI, Y., MIYABAYASHI, K., KOMATSU, T., OWAKI, A., BABA, T., SHIMA, Y., KIDOKORO, T., KANAI, Y., SCHEDL, A., WILHELM, D., KOOPMAN, P., OKUNO, Y. & MOROHASHI, K. 2012. Cbx2, a polycomb group gene, is required for Sry gene expression in mice. *Endocrinology,* 153**,** 913-24.

KENNEDY, M. W., CHALAMALASETTY, R. B., THOMAS, S., GARRIOCK, R. J., JAILWALA, P. & YAMAGUCHI, T. P. 2016. Sp5 and Sp8 recruit β-catenin and Tcf1-Lef1 to select enhancers to activate Wnt target gene transcription. *Proc Natl Acad Sci U S A,* 113**,** 3545-50.

KHAN, A., FORNES, O., STIGLIANI, A., GHEORGHE, M., CASTRO-MONDRAGON, J. A., VAN DER LEE, R., BESSY, A., CHÈNEBY, J., KULKARNI, S. R., TAN, G., BARANASIC, D., ARENILLAS, D. J., SANDELIN, A., VANDEPOELE, K., LENHARD, B., BALLESTER, B., WASSERMAN, W. W., PARCY, F. & MATHELIER, A. 2018. JASPAR 2018: update of the open-access database of transcription factor binding profiles and its web framework. *Nucleic Acids Res,* 46**,** D260-D266.

KIM, B., KIM, Y., SAKUMA, R., HUI, C. C., RÜTHER, U. & JORGENSEN, J. S. 2011. Primordial germ cell proliferation is impaired in Fused Toes mutant embryos. *Developmental Biology,* 349**,** 417-426.

KIM, Y., KOBAYASHI, A., SEKIDO, R., DINAPOLI, L., BRENNAN, J., CHABOISSIER, M. C., POULAT, F., BEHRINGER, R. R., LOVELL-BADGE, R. & CAPEL, B. 2006. Fgf9 and Wnt4 act as antagonistic signals to regulate mammalian sex determination. *PLoS Biol,* 4**,** e187.

KNUTSON, S. K., KAWANO, S., MINOSHIMA, Y., WARHOLIC, N. M., HUANG, K. C., XIAO, Y., KADOWAKI, T., UESUGI, M., KUZNETSOV, G., KUMAR, N., WIGLE, T. J., KLAUS, C. R., ALLAIN, C. J., RAIMONDI, A., WATERS, N. J., SMITH, J. J., PORTER-SCOTT, M., CHESWORTH, R., MOYER, M. P., COPELAND, R. A., RICHON, V. M., UENAKA, T., POLLOCK, R. M., KUNTZ, K. W., YOKOI, A. & KEILHACK, H. 2014. Selective inhibition of EZH2 by EPZ-6438 leads to potent antitumor activity in EZH2-mutant non-Hodgkin lymphoma. *Mol Cancer Ther,* 13**,** 842-54.

KOBAYASHI, D., KOBAYASHI, M., MATSUMOTO, K., OGURA, T., NAKAFUKU, M. & SHIMAMURA, K. 2002. Early subdivisions in the neural plate define distinct competence for inductive signals. *Development,* 129**,** 83-93.

KORINEK, V., BARKER, N., MORIN, P. J., VAN WICHEN, D., DE WEGER, R., KINZLER, K. W., VOGELSTEIN, B. & CLEVERS, H. 1997. Constitutive transcriptional activation by a beta-catenin-Tcf complex in APC-/- colon carcinoma. *Science,* 275**,** 1784-7.

KUMAR, M., CAMLIN, N. J., HOLT, J. E., TEIXEIRA, J. M., MCLAUGHLIN, E. A. & TANWAR, P. S. 2016. Germ cell specific overactivation of WNT/βcatenin signalling has no effect on folliculogenesis but causes fertility defects due to abnormal foetal development. *Sci Rep,* 6**,** 27273.

KUROKI, S., MATOBA, S., AKIYOSHI, M., MATSUMURA, Y., MIYACHI, H., MISE, N., ABE, K., OGURA, A., WILHELM, D., KOOPMAN, P., NOZAKI, M., KANAI, Y., SHINKAI, Y. & TACHIBANA, M. 2013. Epigenetic regulation of mouse sex determination by the histone demethylase Jmjd1a. *Science,* 341**,** 1106-9.

KUROKI, S., OKASHITA, N., BABA, S., MAEDA, R., MIYAWAKI, S., YANO, M., YAMAGUCHI, M., KITANO, S., MIYACHI, H., ITOH, A., YOSHIDA, M. & TACHIBANA, M. 2017. Rescuing the aberrant sex development of H3K9 demethylase Jmjd1a-deficient mice by modulating H3K9 methylation balance. *PLoS Genet,* 13**,** e1007034.

LIN, R. S., JIMENEZ-MOVILLA, M. & DEAN, J. 2014. Figla-Cre transgenic mice expressing myristoylated EGFP in germ cells provide a model for investigating perinatal oocyte dynamics. *PLoS One,* 9**,** e84477.

LIU, C.-F., BINGHAM, N., PARKER, K. & YAO, H. H. C. 2009. Sex-specific roles of beta-catenin in mouse gonadal development. *Human molecular genetics,* 18**,** 405-17.

LIVAK, K. J. & SCHMITTGEN, T. D. 2001. Analysis of relative gene expression data using real-time quantitative PCR and the 2(-Delta Delta C(T)) Method. *Methods,* 25**,** 402-8.

LOVRICS, A., GAO, Y., JUHÁSZ, B., BOCK, I., BYRNE, H. M., DINNYÉS, A. & KOVÁCS, K. A. 2014. Boolean modelling reveals new regulatory connections between transcription factors orchestrating the development of the ventral spinal cord. *PLoS One,* 9**,** e111430.

MAATOUK, D. M., DINAPOLI, L., ALVERS, A., PARKER, K. L., TAKETO, M. M. & CAPEL, B. 2008. Stabilization of β-catenin in XY gonads causes male-to-female sex-reversal. *Human Molecular Genetics,* 17**,** 2949-2955.

MAATOUK, D. M., NATARAJAN, A., SHIBATA, Y., SONG, L., CRAWFORD, G. E., OHLER, U. & CAPEL, B. 2017. Genome-wide identification of regulatory elements in Sertoli cells. *Development,* 144**,** 720-730.

MANUYLOV, N. L., SMAGULOVA, F. O., LEACH, L. & TEVOSIAN, S. G. 2008. Ovarian development in mice requires the GATA4-FOG2 transcription complex. *Development (Cambridge, England),* 135**,** 3731-43.

MARTINEAU, J., NORDQVIST, K., TILMANN, C., LOVELL-BADGE, R. & CAPEL, B. 1997. Male-specific cell migration into the developing gonad. *Curr Biol,* 7**,** 958-68.

MATSUMOTO, Y., BUEMIO, A., CHU, R., VAFAEE, M. & CREWS, D. 2013. Epigenetic control of gonadal aromatase (cyp19a1) in temperature-dependent sex determination of red-eared slider turtles. *PLoS One,* 8**,** e63599.

MCMAHON, A. P., ARONOW, B. J., DAVIDSON, D. R., DAVIES, J. A., GAIDO, K. W., GRIMMOND, S., LESSARD, J. L., LITTLE, M. H., POTTER, S. S., WILDER, E. L., ZHANG, P. & PROJECT, G. 2008. GUDMAP: the genitourinary developmental molecular anatomy project. *J Am Soc Nephrol,* 19**,** 667-71.

MORAIS DA SILVA, S., HACKER, A., HARLEY, V., GOODFELLOW, P., SWAIN, A. & LOVELL-BADGE, R. 1996. Sox9 expression during gonadal development implies a conserved role for the gene in testis differentiation in mammals and birds. *Nat Genet,* 14**,** 62-8.

NAILLAT, F., PRUNSKAITE-HYYRYLAINEN, R., PIETILA, I., SORMUNEN, R., JOKELA, T., SHAN, J. & VAINIO, S. J. 2010a. Wnt4/5a signalling coordinates cell adhesion and entry into meiosis during presumptive ovarian follicle development. *Hum Mol Genet,* 19**,** 1539-50.

NAILLAT, F., PRUNSKAITE-HYYRYLÄINEN, R., PIETILÄ, I., SORMUNEN, R., JOKELA, T., SHAN, J. & VAINIO, S. J. 2010b. Wnt4/5a signalling coordinates cell adhesion and entry into meiosis during presumptive ovarian follicle development. *Human Molecular Genetics,* 19**,** 1539-1550.

NAILLAT, F., YAN, W., KARJALAINEN, R., LIAKHOVITSKAIA, A., SAMOYLENKO, A., XU, Q., SUN, Z., SHEN, B., MEDVINSKY, A., QUAGGIN, S. & VAINIO, S. J. 2015. Identification of the genes regulated by Wnt-4, a critical signal for commitment of the ovary. *Experimental Cell Research,* 2.

NAVARRO-MARTÍN, L., VIÑAS, J., RIBAS, L., DÍAZ, N., GUTIÉRREZ, A., DI CROCE, L. & PIFERRER, F. 2011. DNA methylation of the gonadal aromatase (cyp19a) promoter is involved in temperature-dependent sex ratio shifts in the European sea bass. *PLoS Genet,* 7**,** e1002447.

NICOL, B. & YAO, H. H. 2014. Building an ovary: insights into establishment of somatic cell lineages in the mouse. *Sex Dev,* 8**,** 243-51.

PARROTT, B. B., KOHNO, S., CLOY-MCCOY, J. A. & GUILLETTE, L. J. 2014. Differential incubation temperatures result in dimorphic DNA methylation patterning of the SOX9 and aromatase promoters in gonads of alligator (Alligator mississippiensis) embryos. *Biol Reprod,* 90**,** 2.

PETERS, T., DILDROP, R., AUSMEIER, K. & RÜTHER, U. 2000. Organization of mouse Iroquois homeobox genes in two clusters suggests a conserved regulation and function in vertebrate development. *Genome Research,* 10**,** 1453-1462.

PIFERRER, F. 2013. Epigenetics of sex determination and gonadogenesis. *Dev Dyn,* 242**,** 360-70.

SEKIDO, R. & LOVELL-BADGE, R. 2008. Sex determination involves synergistic action of SRY and SF1 on a specific Sox9 enhancer. *Nature,* 453**,** 930-4.

SIRBU, I. O., GRESH, L., BARRA, J. & DUESTER, G. 2005. Shifting boundaries of retinoic acid activity control hindbrain segmental gene expression. *Development,* 132**,** 2611-22.

SVINGEN, T. & KOOPMAN, P. 2013. Building the mammalian testis: origins, differentiation, and assembly of the component cell populations. *Genes Dev,* 27**,** 2409-26.

TOMIZUKA, K., HORIKOSHI, K., KITADA, R., SUGAWARA, Y., IBA, Y., KOJIMA, A., YOSHITOME, A., YAMAWAKI, K., AMAGAI, M., INOUE, A., OSHIMA, T. & KAKITANI, M. 2008. R-spondin1 plays an essential role in ovarian development through positively regulating Wnt-4 signaling. *Human molecular genetics,* 17**,** 1278-91.

UHLENHAUT, N. H., JAKOB, S., ANLAG, K., EISENBERGER, T., SEKIDO, R., KRESS, J., TREIER, A.-C., KLUGMANN, C., KLASEN, C., HOLTER, N. I., RIETHMACHER, D., SCHÜTZ, G., COONEY, A. J., LOVELL-BADGE, R. & TREIER, M. 2009. Somatic sex reprogramming of adult ovaries to testes by FOXL2 ablation. *Cell,* 139**,** 1130-42.

USONGO, M., RIZK, A. & FAROOKHI, R. 2012. ??-Catenin/Tcf signaling in murine oocytes identifies nonovulatory follicles. *Reproduction,* 144**,** 669-676.

VAINIO, S., HEIKKILÄ, M., KISPERT, A., CHIN, N. & MCMAHON, A. P. 1999. Female development in mammals is regulated by Wnt-4 signalling. *Nature,* 397**,** 405-9.

VAN DE WETERING, M., CAVALLO, R., DOOIJES, D., VAN BEEST, M., VAN ES, J., LOUREIRO, J., YPMA, A., HURSH, D., JONES, T., BEJSOVEC, A., PEIFER, M., MORTIN, M. & CLEVERS, H. 1997. Armadillo coactivates transcription driven by the product of the Drosophila segment polarity gene dTCF. *Cell,* 88**,** 789-99.

VAN GALEN, P., VINY, A. D., RAM, O., RYAN, R. J. H., COTTON, M. J., DONOHUE, L., SIEVERS, C., DRIER, Y., LIAU, B. B., GILLESPIE, S. M., CARROLL, K. M., CROSS, M. B., LEVINE, R. L. & BERNSTEIN, B. E. 2016. A Multiplexed System for Quantitative Comparisons of Chromatin Landscapes. *Molecular Cell,* 61**,** 170-180.

YAN, H., WEN, J., ZHANG, T., ZHENG, W., HE, M., HUANG, K., GUO, Q., CHEN, Q., YANG, Y., DENG, G., XU, J., WEI, Z., ZHANG, H., XIA, G. & WANG, C. 2019. Oocyte-derived E-cadherin acts as a multiple functional factor maintaining the primordial follicle pool in mice. *Cell Death Dis,* 10**,** 160.

YAN, M., LI, G. & AN, J. 2017. Discovery of small molecule inhibitors of the Wnt/β-catenin signaling pathway by targeting β-catenin/Tcf4 interactions. *Exp Biol Med (Maywood),* 242**,** 1185-1197.

Figures

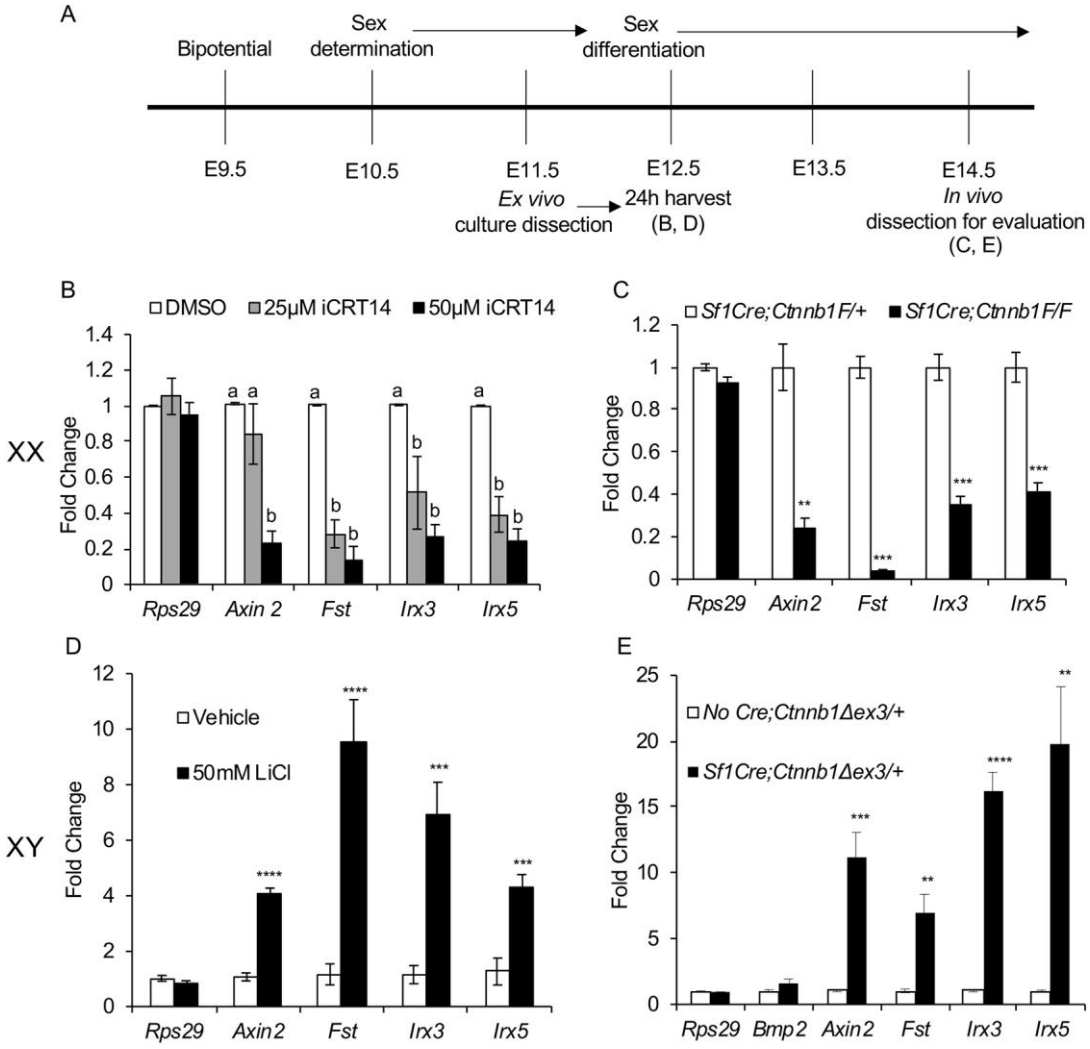

Figure 1: *β-catenin activity correlates with Irx3 and Irx5 expression*

(**A**) Experimental timeline for *ex vivo* and *in vivo* analysis of *β-catenin* manipulation in mouse gonads. Gonads first appear at embryonic day (E) 9.5 and sex determination commences by E10.5. (**B**) *Ex vivo:* RNA analysis from wild type E11.5 ovaries (XX) that were cultured for 24 hours in 20μL media containing either vehicle (DMSO), 25μM, or 50μM iCRT14. (n = 4) One-Way ANOVA, Posthoc Tukey. (**C**) *In vivo:* RNA analysis from E14.5 ovaries (XX) from control (*Sf1Cre;Ctnnb1*$^{F/+}$) and mutant

(*Sf1Cre;Ctnnb1$^{F/F}$)* embryos and subjected to qPCR analysis. (n = 4-5) (**D**) *Ex vivo:* RNA analysis from wild type E11.5 testes (XY) cultured for 24 hours in 20µL media containing either vehicle (water) or 50mM Lithium Chloride (LiCl). (n = 4) (**E**) *In vivo:* RNA analysis from E14.5 testes (XY) from control (No Cre*;Ctnnb1$^{\Delta ex3/+}$*) and mutant (*Sf1Cre;Ctnnb1$^{\Delta ex3/+}$)* embryos and subjected to qPCR analysis. (n = 6) Error bars represent +/- SEM. Student t-test, *p<0.05, **p<0.01, ***p<0.005, ****p<0.001.

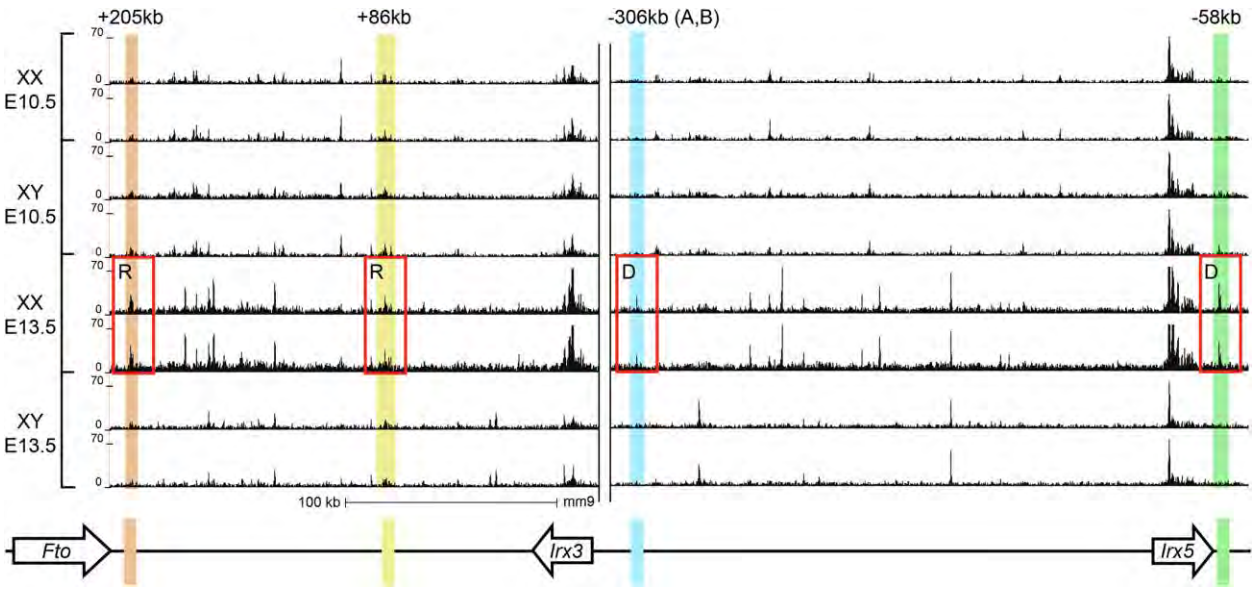

Figure 2: *Open chromatin regions containing TCF/LEF binding motifs are identified in the IrxB locus*

ATAC-seq tracks in isolated somatic cells pre (E10.5) and post (E13.5) sex determination from both female (XX) and male (XY) gonads show four highlighted regions that contain a female specific peak at E13.5 and also includes a TCF/LEF binding motif (TCAAAG) (outlined in boxes). Note that for each Seq analysis, there are duplicate assays presented for each age/sex gonad. Site -305 'A' and 'B' indicate two separate TCF/LEF binding motifs. Each putative site is labeled based on its distance to the *Irx3* promoter *Irx3* and *Irx5* tss' position labeled with red arrow. Genes within the same locus include *Fto* and *Crnde* (lncRNA). Transcription direction is labeled with block arrows. A model of the *IrxB* locus and each putative enhancer site relative to the *Irx3* tss. Color coding for each putative enhancer site is maintained throughout. R=resolved, D=de novo peaks within the E13.5 ovary. ATAC-seq data was taken from Garcia-Moreno et al., 2019a.

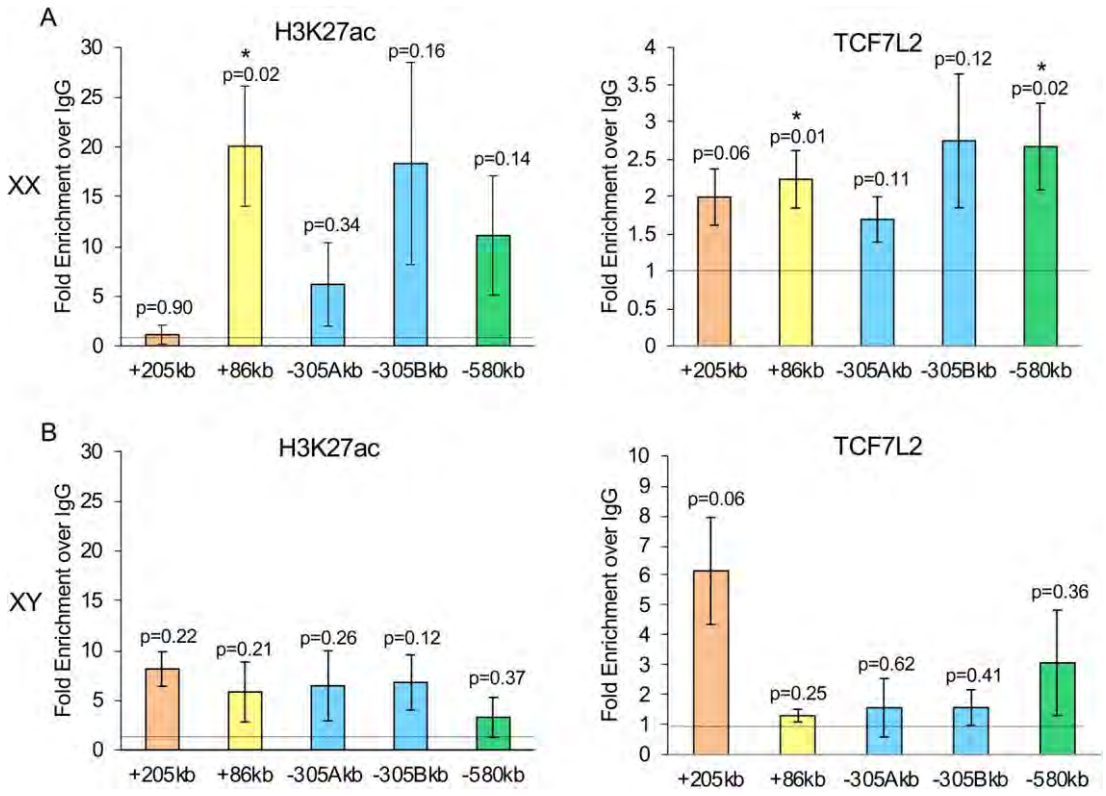

Figure 3: *Ovary-specific β-catenin responsive enhancer sites reside within the IrxB locus*

(**A**) H3K27ac (active enhancer marker) (left panel) and β-catenin binding partner TCF7L2 (right panel) chromatin immunoprecipitation (ChIP) of E14.5 ovaries (XX) from wild-type mice. (**B**) ChIP using the same markers in E14.5 testes (XY). H3K27ac (left panel) and TCF7L2 (right panel). Data are represented as fold change over IgG, which is normalized to 1. Data are presented as the average +/- SEM. Student t-test. Female (XX) n = 5-9, Male (XY) n = 3-4 biological replicates.

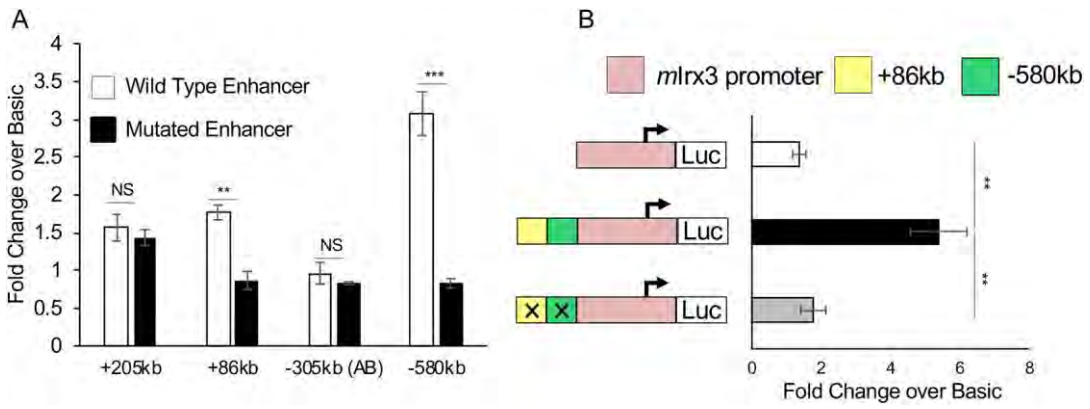

Figure 4: *Constitutively active β-catenin defines +86kb and -580kb as Wnt responsive enhancers within the Irx3/5 locus.*

(**A**) Luciferase reporter plasmids containing wild type and mutated DNA sequences of each putative enhancer site were transfected into HEK293 cells along with CMV-S37A, an expression vector that encodes a constitutively active form of β-catenin. Test plasmids were normalized to pGL3 Basic activity; n = 3 individual experiments, each performed in triplicate.

(**B**) -1634/+446bp m*Irx3* pGL3, +86kb WT;-580kb WT; -1634/+446bp m*Irx3* pGL3, or +86kb MUT; -580kb MUT; -1634/+446bp m*Irx3* pGL3 were transfected into HEK293 cells along with a constitutively active β-catenin expression vector, CMV-S37A. Data are presented as the average +/- SEM; n = 4-5 individual experiments, each performed in triplicate. Student t-test, **p<0.01, ***p<0.005

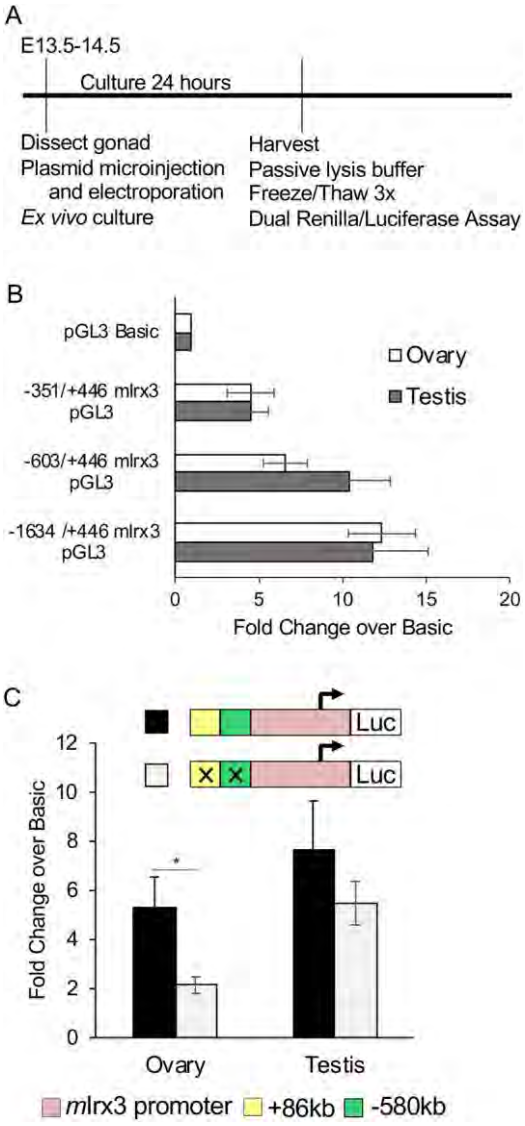

Figure 5: *+86kb and -580kb enhancers promote β-catenin specific activity in transfected fetal ovaries*

(**A**) Experimental timeline for gonad dissection, transfection via microinjection and electroporation, culture, and harvest for dual luciferase assay. (**B**) *Ex vivo* transfections in ovary (white bars) versus testes (dark bars) of luciferase reporter vectors containing increasing sequence lengths of the mouse *Irx3* promoter compared to the empty pGL3 Basic control reporter vector. -1634/+446 testis n = 7,

ovary n = 8. -603/+446 testis n = 11, ovary n = 8. -351/+446 testis and ovary n = 5. (**C**) *Ex vivo* transfections in ovary (white bars) versus testes (black bars) of +86kb WT; -580kb WT; -1634/+446bp m*Irx3* pGL3 or +86kb MUT; -580kb MUT; -1634/+446bp m*Irx3* pGL3. All data is represented as the fold change over pGL3 Basic. WT vector ovary n = 9, WT vector testis n = 13, MUT vector ovary n = 3, MUT vector testis n = 7. Data are represented as the average +/- SEM. Student t-test, *p<0.05.

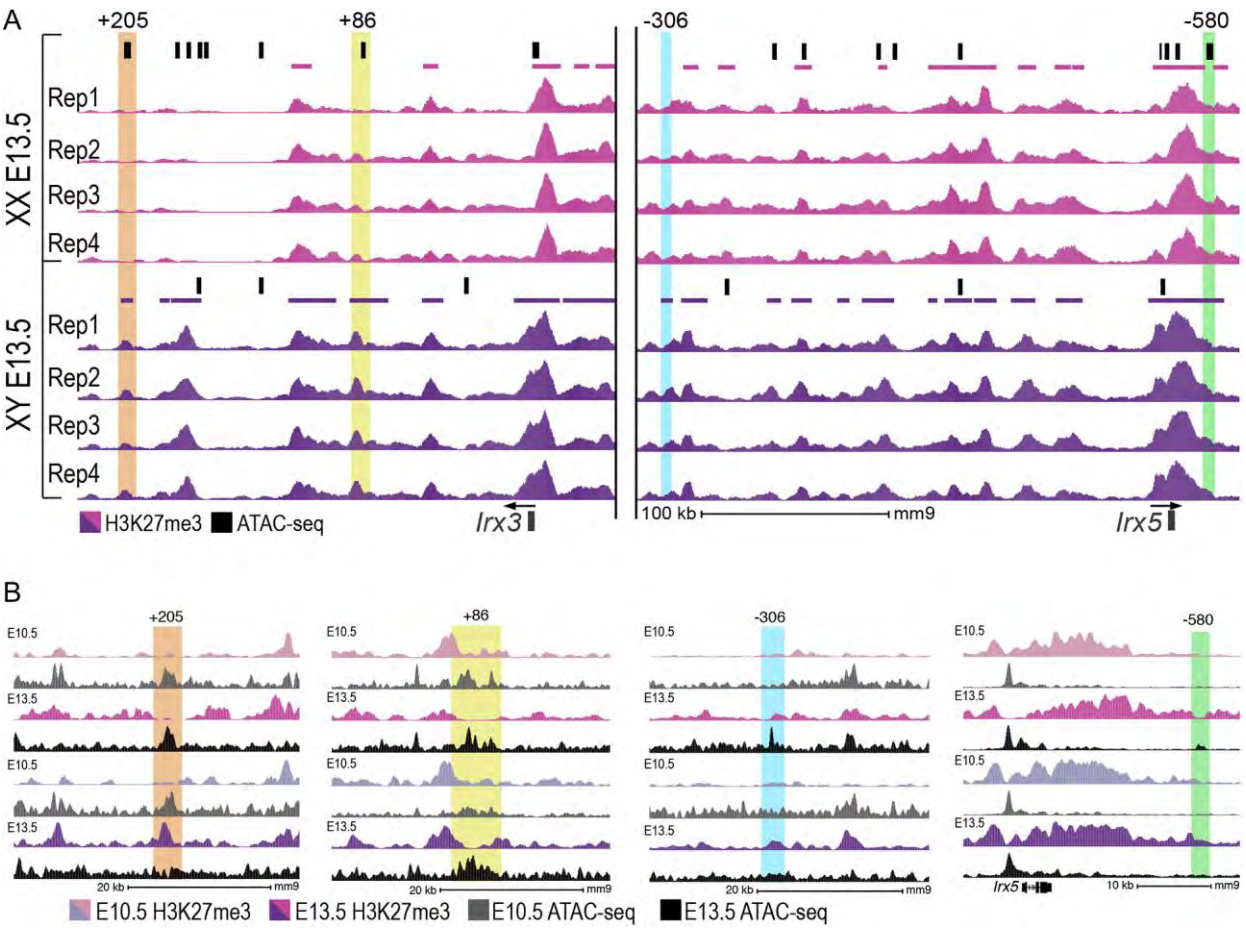

Figure 6: *+86kb and -580kb sites are repressed in the fetal testis*

(A) Genome browser tracks showing four biological replicates of H3K27me3 ChIP-seq in purified E13.5 XX (pink) and XY (purple) gonadal supporting cells. The top 2 replicates are taken from Garcia-Moreno et al., 2019b, the bottom two replicates were performed in this study. Bold lines above tracks (pink-XX, purple-XY) represent significant enrichment whe compared to flanking regions as determined by HOMER. ATAC-seq tracks (from Garcia-Moreno et al., 2019a) are presented as black boxes above ChIP-seq tracks. (B) Genome browser tracks at each seleted site (highlighted) showing H3K27me3 ChIP-seq in E10.5 XX (light pink) and XY (light purple), and E13.5 XX (dark pink) and XY (dark purple) gonadal supporting cells. ATAC-seq from

purified E10.5 (grey) and E13.5 (black) XX and XY somatic cells are also shown (Seq datasets taken from Garcia-Moreno et al., 2019a and Garcia-Moreno et al., 2019b).

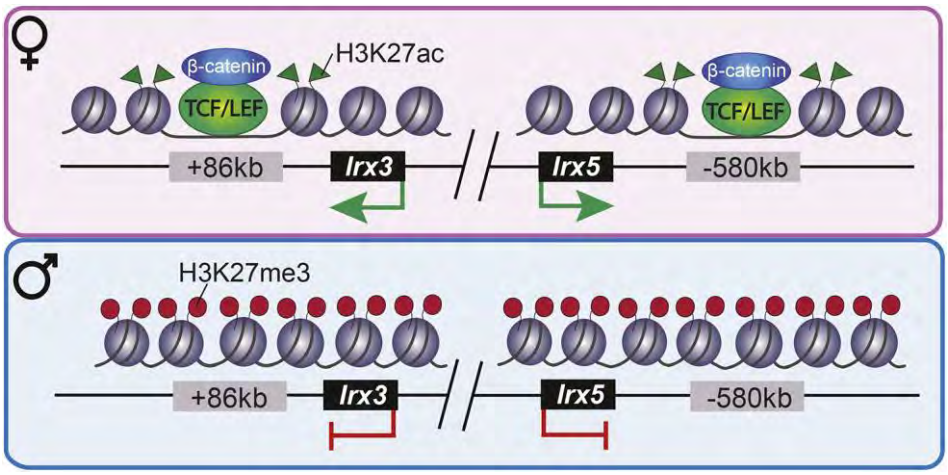

Figure 7: *Working model of β-catenin/TCF binding and epigenetic regulation of Irx3 and Irx5*

Top Panel: In the ovary, H3K27ac (green triangles) mark active enhancer elements +86kb and -580kb in conjunction with β-catenin/TCF binding to promote *Irx3* and *Irx5* transcription. Bottom panel: In the testis, repressive histone mark H3K27me3 is present at the +86kb and -580kb sequences, restricting *Irx3* and *Irx5* transcription.

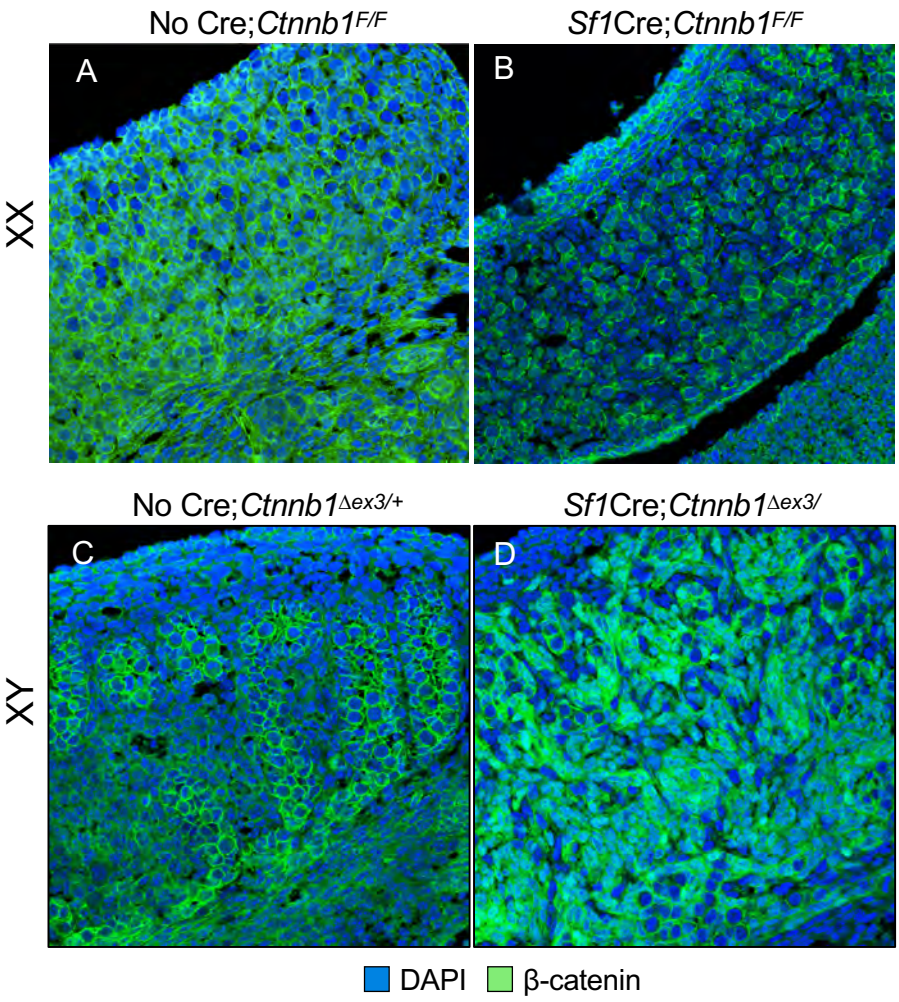

Figure S1: *Somatic cell manipulation of β-catenin in the developing gonad*
E14.5 (**A**) Control ovary (No Cre;*Ctnnb1*$^{F/F}$) and (**B**) mutant ovary (*Sf1*Cre;*Ctnnb1*$^{F/F}$) β-catenin green, DAPI blue. The remaining β-catenin in the mutant ovary resides in the germ cell membrane. E14.5 (**C**) Control testis (No Cre;*Ctnnb1*$^{\Delta ex3/+}$) and (**D**) mutant testis (*Sf1*Cre;*Ctnnb1*$^{\Delta ex3/+}$) β-catenin green, DAPI blue. β-catenin is highly stabilized in the mutant testis.

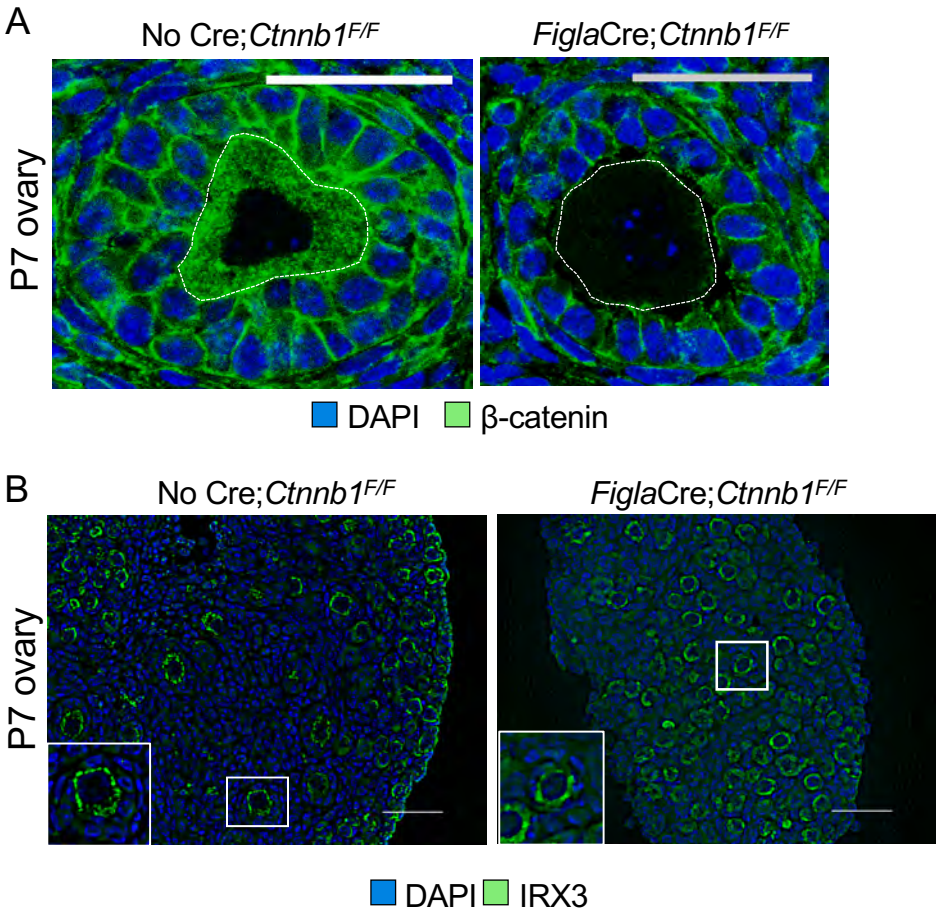

Figure S2: *FiglaCre targeted loss of β-catenin does not affect IRX3 expression in oocytes*

(**A**) Immunofluorescence image of a primary/transitioning follicle in a P7 ovary showing that β-catenin is knocked out specifically in the oocyte. No Cre;*Ctnnb1*$^{F/F}$ (control, left panel). *Figla*Cre*;Ctnnb1*$^{F/F}$ (mutant, right panel). DAPI (blue) and β-catenin (green), White dotted lines outline the membrane of the germ cell. (**B**) IHC images of P7 ovaries for DAPI (blue) and IRX3 (green). No difference was observed in IRX3 staining between the oocytes of the control and mutant ovaries, including growing follicles (inset). Timing starting at secondary follicles is consistent with the onset of transcriptional activity of β-catenin in postnatal ovaries as reported by Usongo *et al.* 2012. Scale bars set to 50μm.

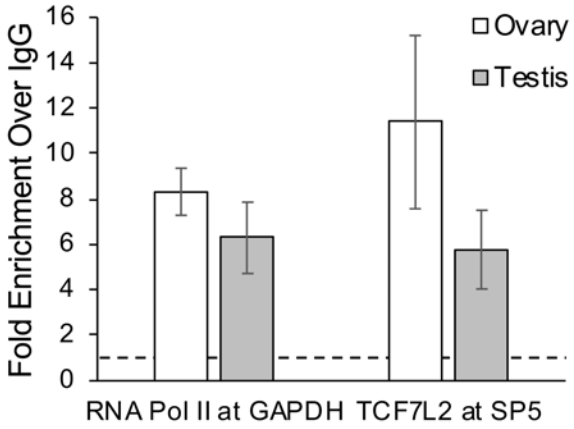

Figure S3: *Chromatin Immunoprecipitation controls*
RNA Pol II is enriched at the GAPDH promoter and TCF7L2 is enriched at the SP5 promoter in both ovaries and testes

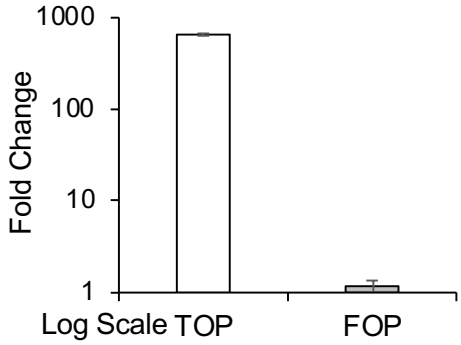

Figure S4: *Validation of β-catenin specific responsiveness for CMV-S37A expression vector*
TOPflash and FOPflash constructs were co-transfected with 50ng/well CMV-EGFP or CMV-S37A and normalized to pGL3Basic. Only TOPflash co-transfected with CMV-S37A showed a specific and robust increase in luciferase expression.

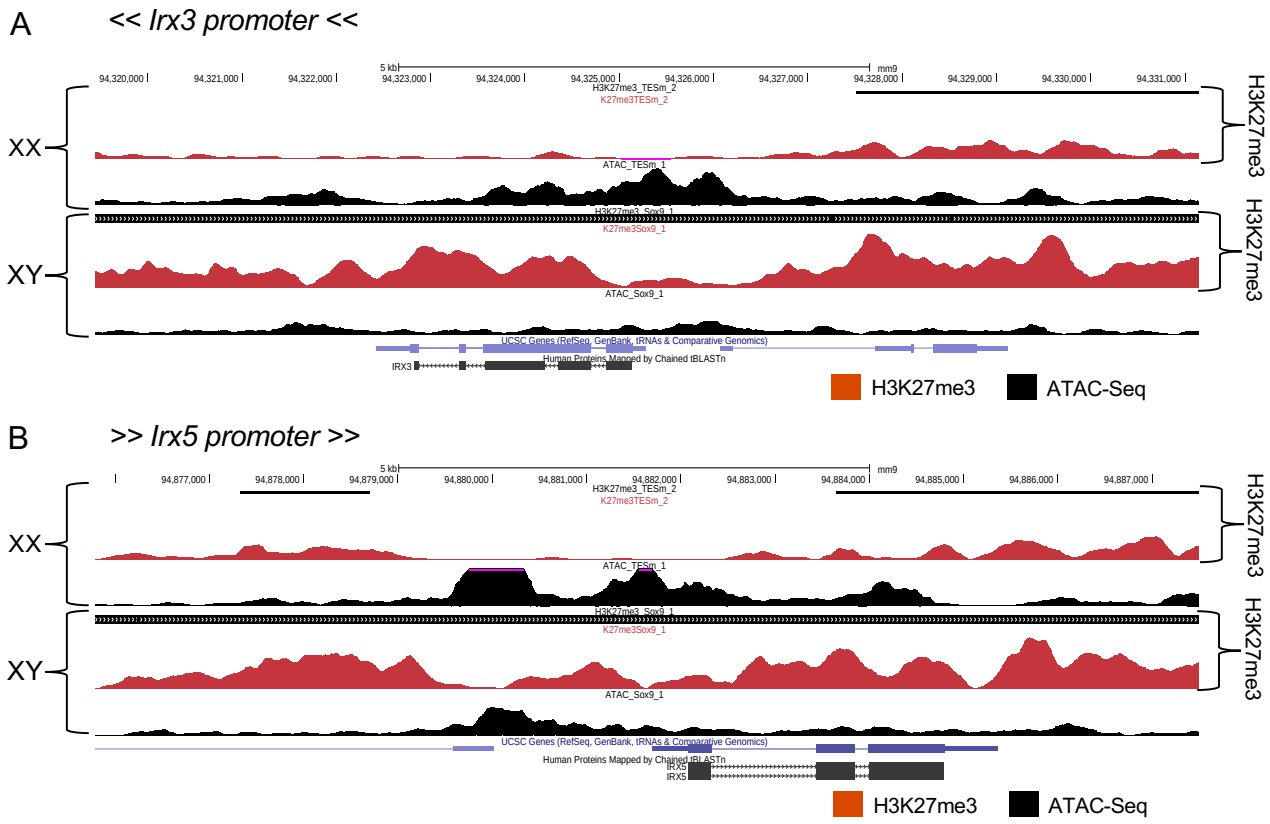

Figure S5: *Epigenetic marks on Irx3 and Irx5 promoters*
H3K27me3 (red peaks and back solid lines) and open chromatin sites (ATAC-Seq, black peaks) are shown for *Irx3* (**C**) and *Irx5* (**D**) promoters in male and female somatic cell populations. Arrows in label match the direction for coding sequences of each gene. ATAC-Seq peaks are enriched while there is a paucity of H3K27me3 peaks in XX samples. Black bars represent regions of significant enrichment when compared to flanking regions as determined by HOMER, thicker lines represent increased enrichment. Black bars are absent in both proximal promoter regions in XX samples.

Site Label	Forward Primer		Reverse Primer	Total insert length
+205kb	5'-GCGCGGTACCTCACCTGGTAACTTTGTGCTGT-3'		5'-GCGCCTCGAGCCAAGGCTTCCGGTATCAGC-3'	108bp
+86kb	5'-GCGCGGTACCTTCCCTTTCCTATTTGTTCAGAAG-3'		5'-GCGCCTCGAGTTCCCTCGGCTGACAGAG-3'	59bp
-305AB kb	5'-GCGCGGTACCGGTTTCAAAAAGCCCAAGTG-3'		5'-GCGCCTCGAGTTATTTCTCTCTTTCTCTCTCTCCA-3'	250bp
-580kb	5'-GCGCGGTACCCCGCCATGATAGGAGTCAAC-3'		5'-GCGCCTCGAGGGCAGCCCTTTGTAAATGTT-3'	89bp
Mutation Site	**+205kb**	**+86kb**	**-305kb (AB)**	**-580kb**
Wild Type Sequence	GTTCAAAGGC	GTTCAAAGCG	(A) GTTCAAAGTC (B) TTTCAAAGGG	CATCAAAGAC
Mutated Sequence	GT**C**CAAAGGC	GT**C**CAAAGCG	(A) GT**C**CAAAGTC (B) TT**C**CAAAGGG	CA**C**CAAAGAC

Table S1: Individual potential enhancer sites containing TCF/LEF motif were cloned into the pGL3 Basic backbone using KpnI and XhoI. Primer sequences listed above and the insert size. DNA was generated by PCR with mouse genomic DNA. Wild type and mutated TCF/LEF binding motif for each enhancer site. The mutated base pair is in bold.

Supplementary Table S2: Real-time qPCR primer sequences

Gene	Forward Primer	Reverse Primer
36B4	5’ – CGACCTGGAAGTCCAACTAC – 3’	5’ – ATCTGCTGCATCTGCTTG - 3’
Gapdh	5’ – TTCACCACCATGGAGAAGGC – 3’	5’ – GGCATGGACTGTGGTCATGA – 3’
Rps29	5' - TGAAGGCAAGATGGGTCAC - 3'	3' - GCACATGTTCAGCCCGTATT - 5'
Axin2	5’ – CCAGGCTGGAGAAACTGAAACT - 3'	5’ – CCTGCTCAGACCCCTCCTTT - 3'
Fst	5' - AAAACCTACCGCAACGAATG - 3'	5' - TTCAGAAGAGGAGGGCTCTG - 3'
Bmp2	5’ – CGGACTGCGGTCTCCTAA – 3’	5’ – GGGGAAGCAGCAACACTAGA – 3’
Irx3	5' - CGCCTCAAGAAGGAGAACAAGA - 3'	5' - CGCTCGCTCCCATAAGCAT - 3'
Irx5	5' - GGCTACAACTCGCACCTCCA - 3'	5' - CCAAGGAACCTGCCATACCG - 3'

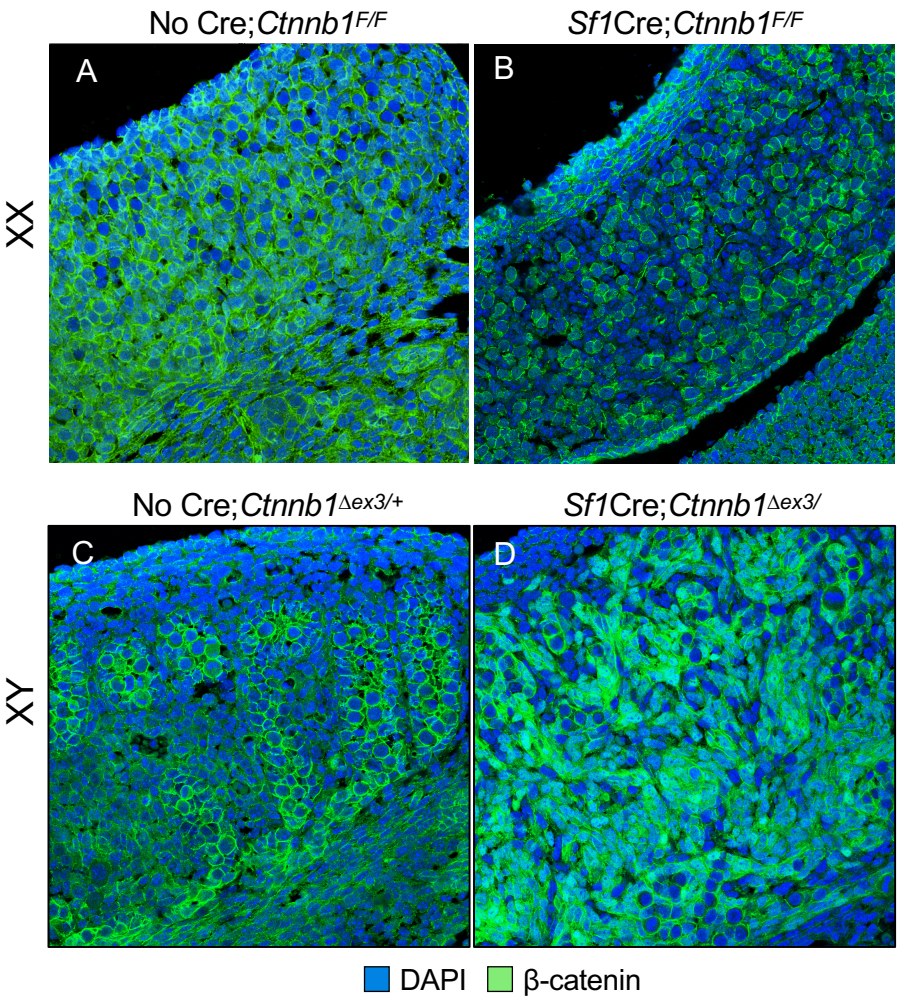

Figure S1: *Somatic cell manipulation of β-catenin in the developing gonad* E14.5 (**A**) Control ovary (No Cre;*Ctnnb1*$^{F/F}$) and (**B**) mutant ovary (*Sf1*Cre;*Ctnnb1*$^{F/F}$) β-catenin green, DAPI blue. The remaining β-catenin in the mutant ovary resides in the germ cell membrane. E14.5 (**C**) Control testis (No Cre;*Ctnnb1*$^{\Delta ex3/+}$) and (**D**) mutant testis (*Sf1*Cre;*Ctnnb1*$^{\Delta ex3/+}$) β-catenin green, DAPI blue. β-catenin is highly stabilized in the mutant testis.

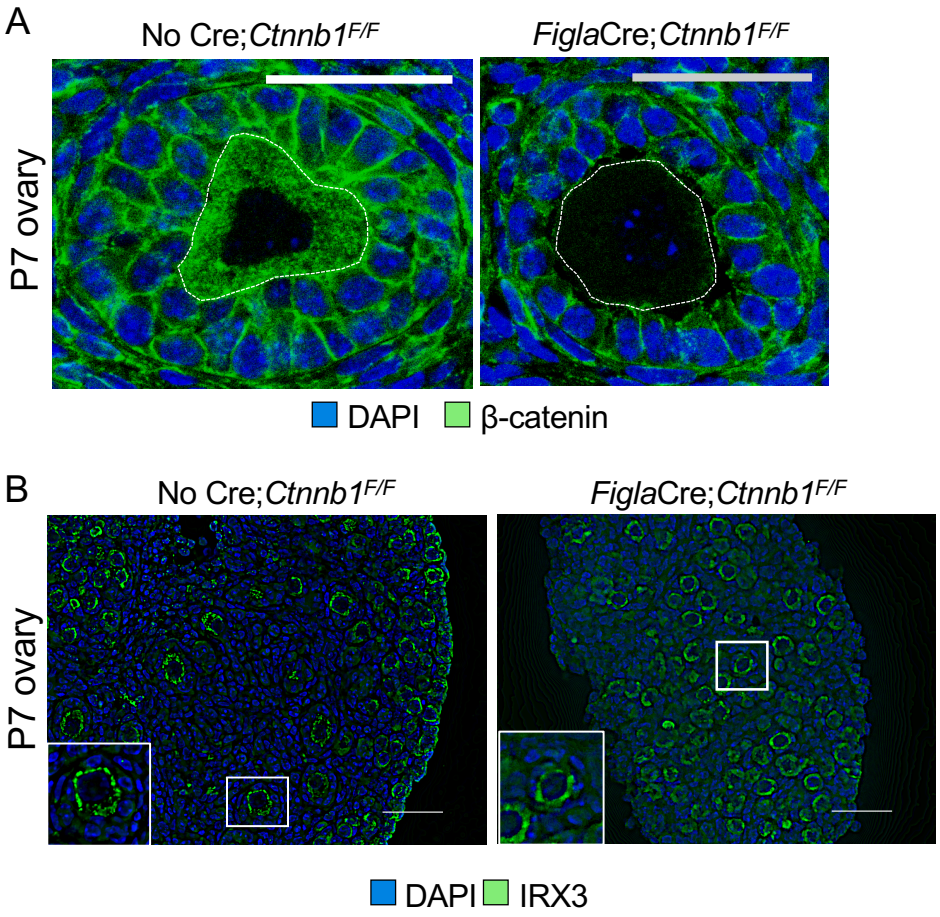

Figure S2: *FiglaCre targeted loss of β-catenin does not affect IRX3 expression in oocytes*

(**A**) Immunofluorescence image of a primary/transitioning follicle in a P7 ovary showing that β-catenin is knocked out specifically in the oocyte. No Cre;*Ctnnb1*$^{F/F}$ (control, left panel). *Figla*Cre*;Ctnnb1*$^{F/F}$ (mutant, right panel). DAPI (blue) and β-catenin (green), White dotted lines outline the membrane of the germ cell. (**B**) IHC images of P7 ovaries for DAPI (blue) and IRX3 (green). No difference was observed in IRX3 staining between the oocytes of the control and mutant ovaries, including growing follicles (inset). Timing starting at secondary follicles is consistent with the onset of transcriptional activity of β-catenin in postnatal ovaries as reported by Usongo *et al.* 2012. Scale bars set to 50μm.

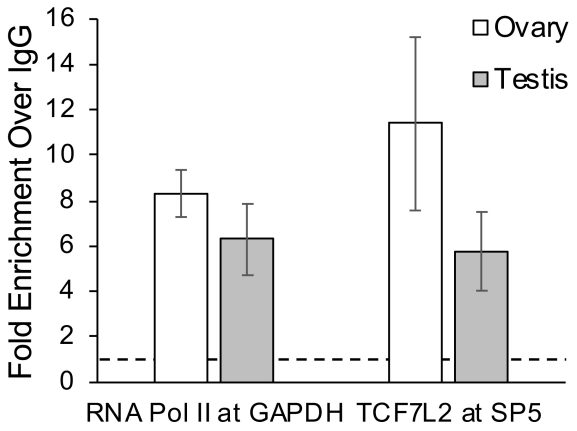

Figure S3: *Chromatin Immunoprecipitation controls*
RNA Pol II is enriched at the GAPDH promoter and TCF7L2 is enriched at the SP5 promoter in both ovaries and testes

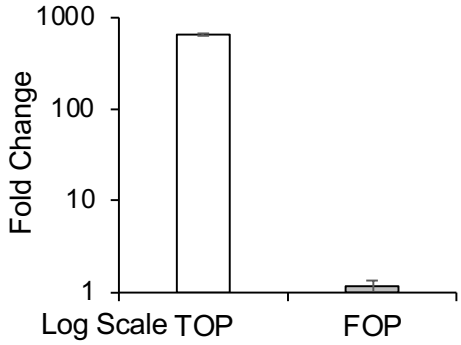

Figure S4: *Validation of β-catenin specific responsiveness for CMV-S37A expression vector*
TOPflash and FOPflash constructs were co-transfected with 50ng/well CMV-EGFP or CMV-S37A and normalized to pGL3Basic. Only TOPflash co-transfected with CMV-S37A showed a specific and robust increase in luciferase expression.

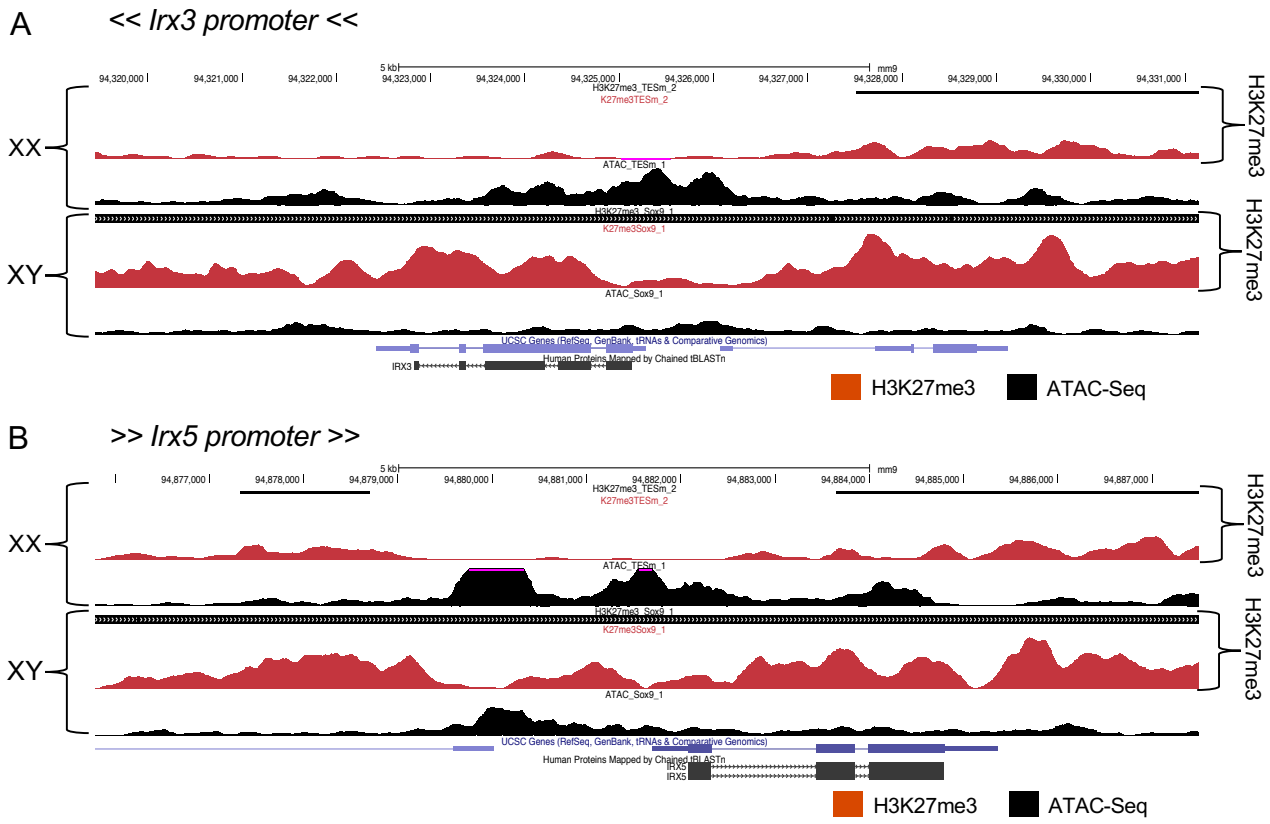

Figure S5: *Epigenetic marks on Irx3 and Irx5 promoters*
H3K27me3 (red peaks and back solid lines) and open chromatin sites (ATAC-Seq, black peaks) are shown for *Irx3* (**C**) and *Irx5* (**D**) promoters in male and female somatic cell populations. Arrows in label match the direction for coding sequences of each gene. ATAC-Seq peaks are enriched while there is a paucity of H3K27me3 peaks in XX samples. Black bars represent regions of significant enrichment when compared to flanking regions as determined by HOMER, thicker lines represent increased enrichment. Black bars are absent in both proximal promoter regions in XX samples.

Site Label	Forward Primer		Reverse Primer	Total insert length
+205kb	5'-GCGCGGTACCTCACCTGGTAACTTTGTGCTGT-3'		5'-GCGCCTCGAGCCAAGGCTTCCGGTATCAGC-3'	108bp
+86kb	5'-GCGCGGTACCTTCCCTTTCCTATTTGTTCAGAAG-3'		5'-GCGCCTCGAGTTCCCTCGGCTGACAGAG-3'	59bp
-305AB kb	5'-GCGCGGTACCGGTTTCAAAAAGCCCAAGTG-3'		5'-GCGCCTCGAGTTATTTCTCTCTTTCTCTCTCTCCA-3'	250bp
-580kb	5'-GCGCGGTACCCCGCCATGATAGGAGTCAAC-3'		5'-GCGCCTCGAGGGCAGCCCTTTGTAAATGTT-3'	89bp
Mutation Site	**+205kb**	**+86kb**	**-305kb (AB)**	**-580kb**
Wild Type Sequence	GTTCAAAGGC	GTTCAAAGCG	(A) GTTCAAAGTC (B) TTTCAAAGGG	CATCAAAGAC
Mutated Sequence	GT**C**CAAAGGC	GT**C**CAAAGCG	(A) GT**C**CAAAGTC (B) TT**C**CAAAGGG	CA**C**CAAAGAC

Table S1: Individual potential enhancer sites containing TCF/LEF motif were cloned into the pGL3 Basic backbone using KpnI and XhoI. Primer sequences listed above and the insert size. DNA was generated by PCR with mouse genomic DNA. Wild type and mutated TCF/LEF binding motif for each enhancer site. The mutated base pair is in bold.

Supplementary Table S2: Real-time qPCR primer sequences

Gene	Forward Primer	Reverse Primer
36B4	5’ – CGACCTGGAAGTCCAACTAC – 3’	5’ – ATCTGCTGCATCTGCTTG - 3’
Gapdh	5’ – TTCACCACCATGGAGAAGGC – 3’	5’ – GGCATGGACTGTGGTCATGA – 3’
Rps29	5' - TGAAGGCAAGATGGGTCAC - 3'	3' - GCACATGTTCAGCCCGTATT - 5'
Axin2	5’ – CCAGGCTGGAGAAACTGAAACT - 3'	5’ – CCTGCTCAGACCCCTCCTTT - 3'
Fst	5' - AAAACCTACCGCAACGAATG - 3'	5' - TTCAGAAGAGGAGGGCTCTG - 3'
Bmp2	5’ – CGGACTGCGGTCTCCTAA – 3’	5’ – GGGGAAGCAGCAACACTAGA – 3’
Irx3	5' - CGCCTCAAGAAGGAGAACAAGA - 3'	5' - CGCTCGCTCCCATAAGCAT - 3'
Irx5	5' - GGCTACAACTCGCACCTCCA - 3'	5' - CCAAGGAACCTGCCATACCG - 3'